University of Glasgow

Jefferson Lab
EXPLORING THE NATURE OF MATTER

Nucleon Tomography through Deeply Virtual Compton Scattering @ Jefferson Lab

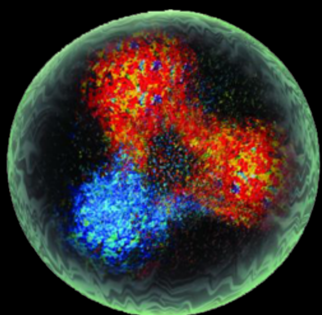

Daria Sokhan

University of Glasgow, UK

and the CLAS Collaboration

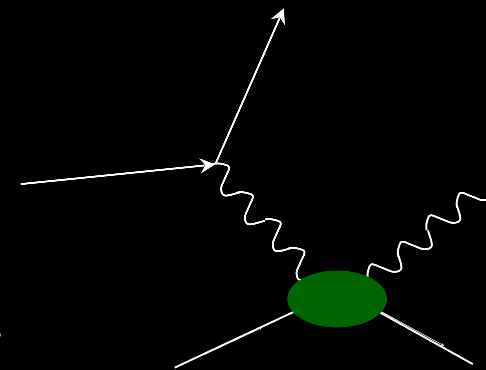

INT 17-3 Workshop: “Hadron Imaging at Jefferson Lab and at a future EIC”

Institute for Nuclear Theory, University of Washington, Seattle

26th September 2017

Intro: nucleon tomography and DVCS

The nucleon deconstructed

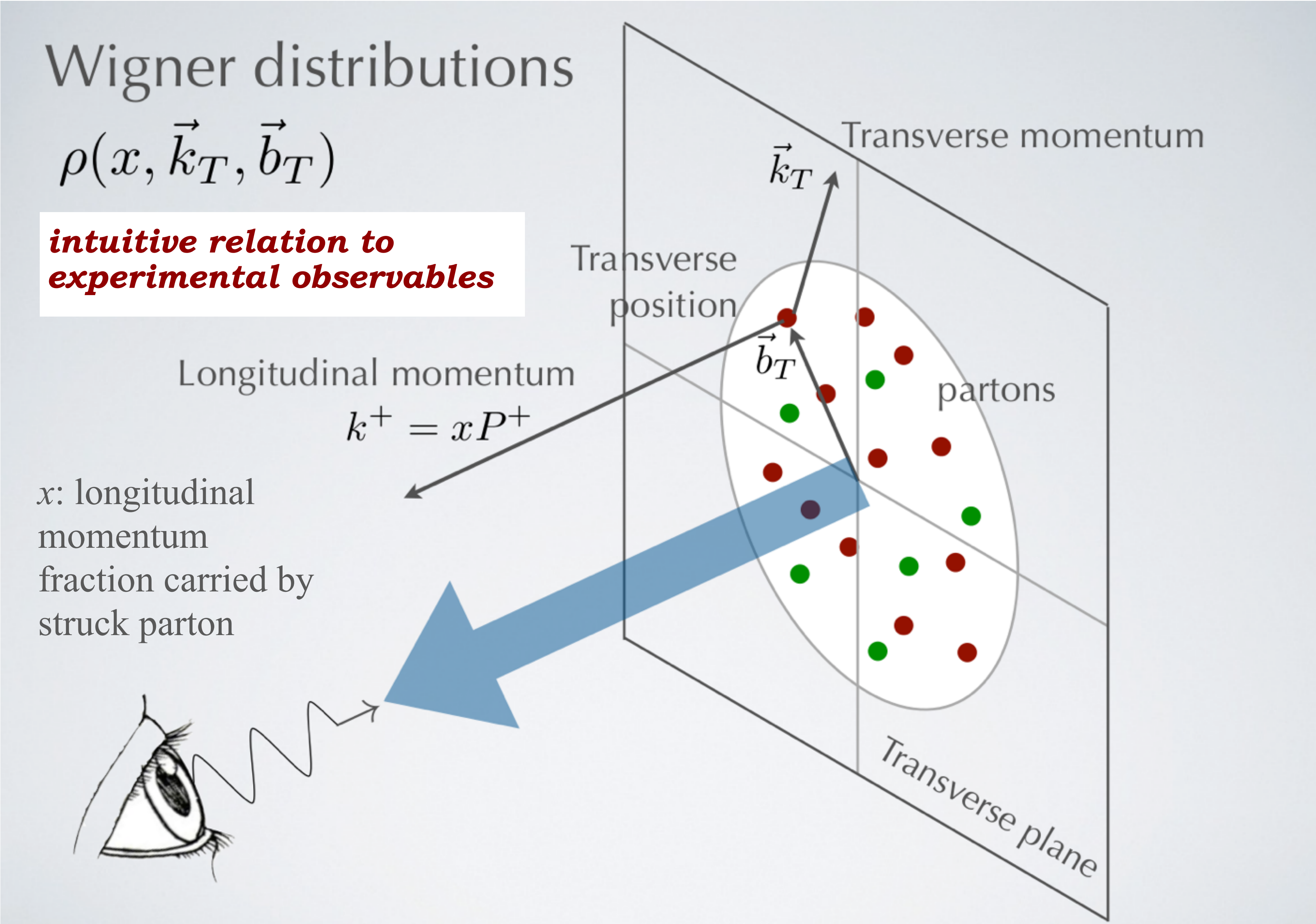

Images of the nucleon

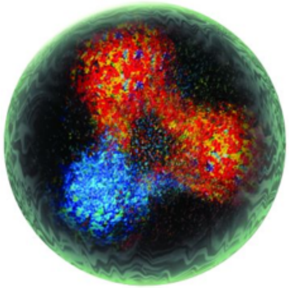

Wigner function:
full phase space parton distribution of the nucleon

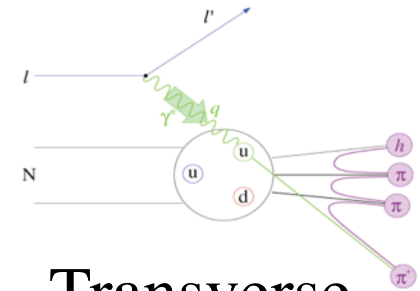

$\int d^2k_T$

$\int d^2b_T$

Transverse Momentum Distributions (TMDs)

Generalised Parton Distributions (GPDs)

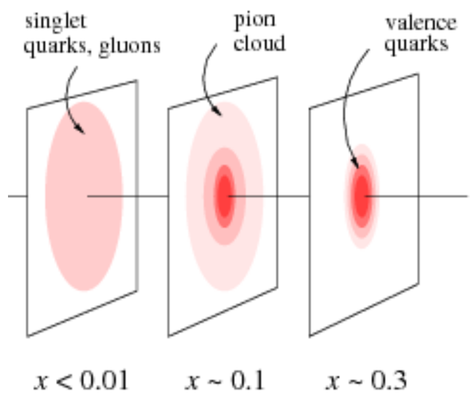

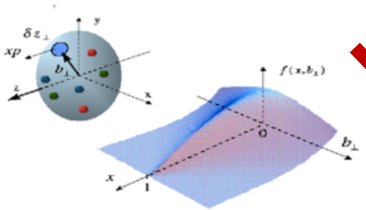

$\int dx$

$\int d^2k_T$

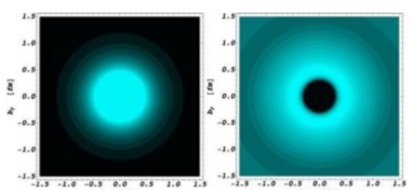

Form Factors
eg: G_E, G_M

Parton Distribution Functions (PDFs)

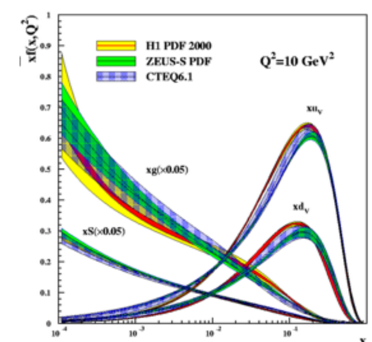

Images of the nucleon

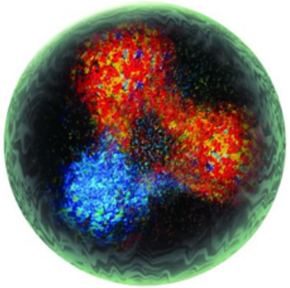

Wigner function:
full phase space parton distribution of the nucleon

$\int d^2 k_T$

$\int d^2 b_T$

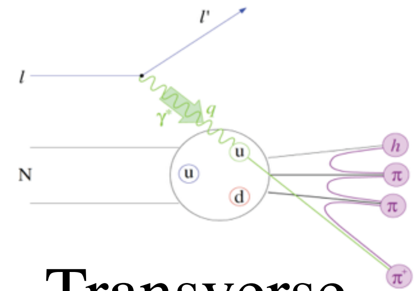

Transverse Momentum Distributions (TMDs)

Generalised Parton Distributions (GPDs)

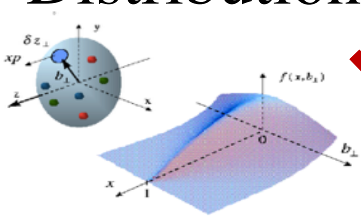

Chihuly Glass Museum, Seattle

$\int dx$

$\int d^2 k_T$

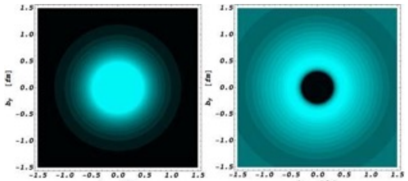

Form Factors
eg: G_{E}, G_M

Parton Distribution Functions (PDFs)

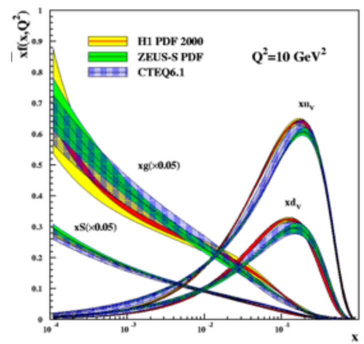

Generalised Parton Distributions

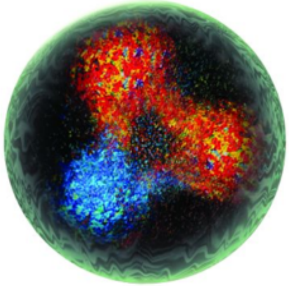

Wigner function:
full phase space parton distribution of the nucleon

$$\int d^2 k_T$$

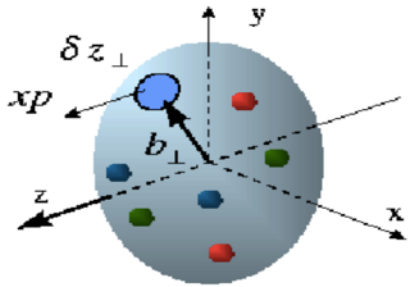

Generalised Parton Distributions (GPDs)

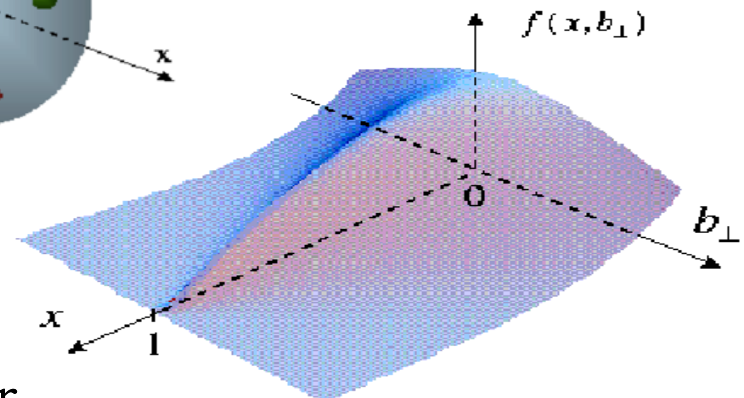

- relate, in the infinite momentum frame, transverse position of partons ($b_\perp$) to their longitudinal momentum (x): **tomography** of the nucleon.

Experimental paths to GPDs

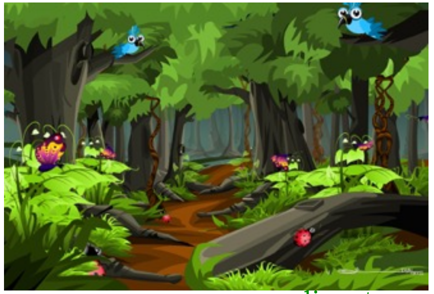
cliparts.co

Accessible in *exclusive* reactions, where all final state particles are detected.

Trodden paths and ones starting to be explored:

- Deeply Virtual Compton Scattering (DVCS)
- Deeply Virtual Meson Production (DVMP)
- Time-like Compton Scattering (TCS)
- Double DVCS

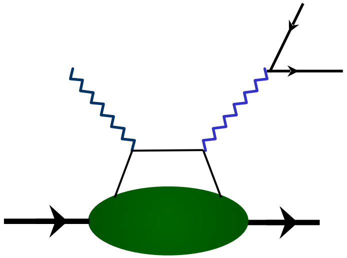
TCS

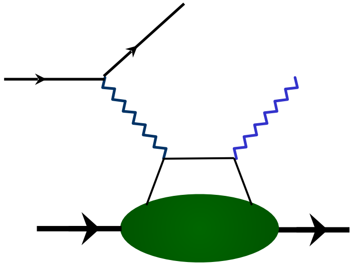
DVCS

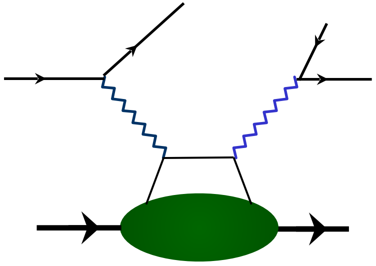
DDVCS

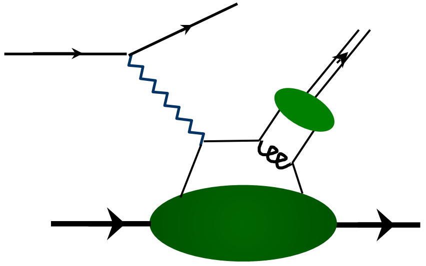
DVMP

Deeply Virtual Compton Scattering

the "golden channel"

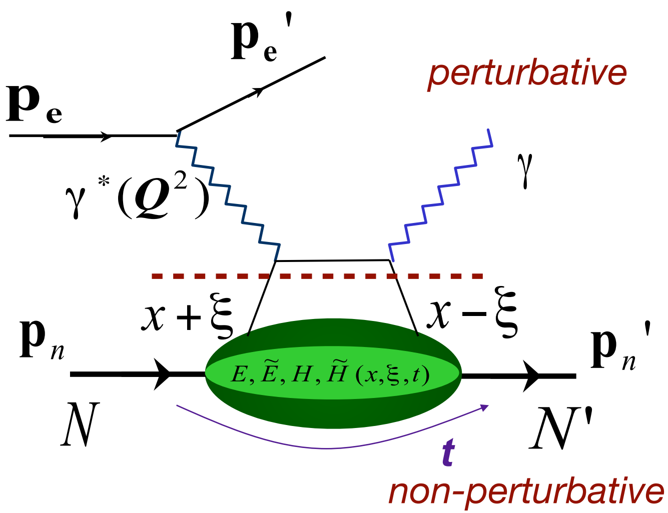

$Q^2 = -(\mathbf{p}_e - \mathbf{p}_e')^2 \qquad t = (\mathbf{p_n} - \mathbf{p_n}')^2$

Bjorken variable: $x_B = \dfrac{Q^2}{2\mathbf{p_n}\cdot\mathbf{q}}$

$x \pm \xi$ *longitudinal momentum fractions of the struck parton*

$$\xi \cong \frac{x_B}{2 - x_B}$$

- At high exchanged Q^2 and low t access to four chiral-even GPDs:

$$E^q, \tilde{E}^q, H^q, \tilde{H}^q(x,\xi,t)$$

- Can be related to PDFs:

$$H(x,0,0) = q(x) \quad \tilde{H}(x,0,0) = \Delta q(x)$$

and form factors:

$$\int_{-1}^{+1} H dx = F_1 \qquad \int_{-1}^{+1} \tilde{H}\, dx = G_A$$

$$\int_{-1}^{+1} E\, dx = F_2 \qquad \int_{-1}^{+1} \tilde{E}\, dx = G_P$$

(Dirac and Pauli) *(axial and pseudo-scalar)*

- Small changes in nucleon transverse momentum allows mapping of transverse structure at large distances.

GPDs and the spin puzzle

- Total angular momentum of a nucleon: $J_N = \frac{1}{2} = \frac{1}{2}\Sigma_q + L_q + J_g$

Only ~ 30% contribution

- Ji's relation:

$$J^q = \frac{1}{2} - J^g = \frac{1}{2}\int_{-1}^{1} x dx \left\{ H^q(x,\xi,0) + E^q(x,\xi,0) \right\}$$

✶Need measurements at low t, across wide Q^2, of a range of observables to extract both H and E.

✶Need flavour separation of GPDs.

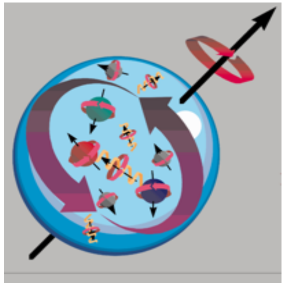

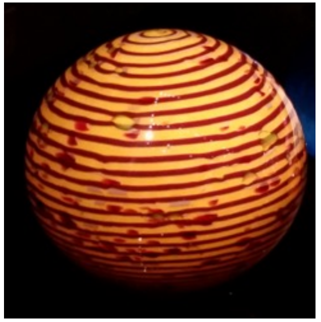

D. Chihuly

Measuring DVCS

✳ Process measured in experiment:

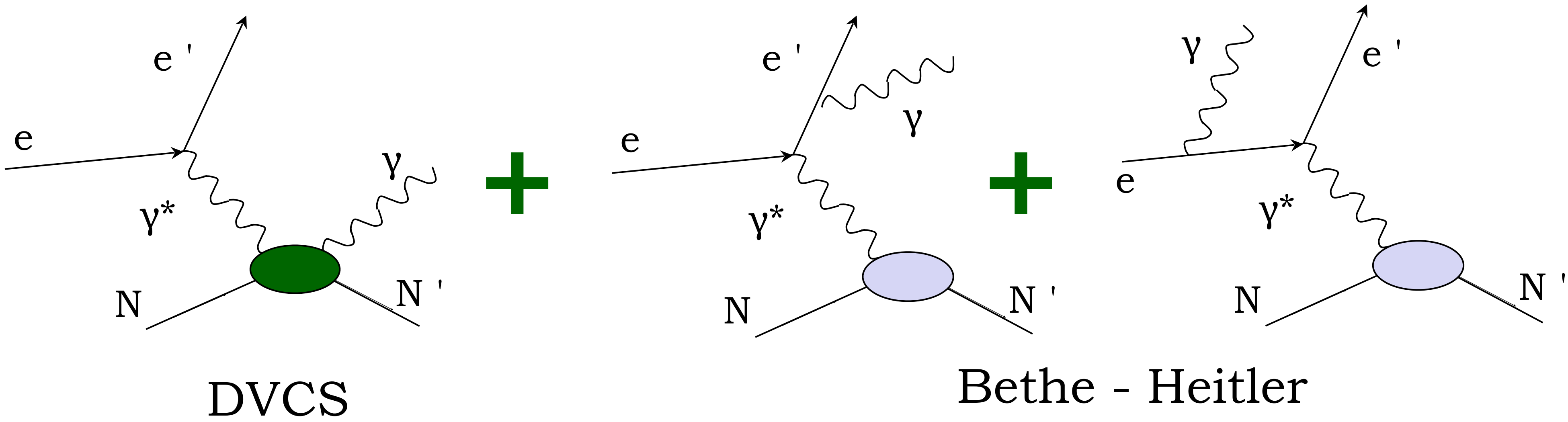

$$d\sigma \propto |T_{DVCS}|^2 + |T_{BH}|^2 + T_{BH}T^*{}_{DVCS} + T_{DVCS}T^*{}_{BH}$$

Amplitude parameterised in terms of Compton Form Factors

Amplitude calculable from elastic Form Factors and QED

Interference term

$$|T_{DVCS}|^2 << |T_{BH}|^2$$

Compton Form Factors in DVCS

Experimentally accessible in DVCS cross-sections and spin asymmetries, eg:

$$A_{LU} = \frac{d\vec{\sigma} - d\overleftarrow{\sigma}}{d\vec{\sigma} + d\overleftarrow{\sigma}} = \frac{\Delta\sigma_{LU}}{d\vec{\sigma} + d\overleftarrow{\sigma}}$$

$$T^{DVCS} \sim \int_{-1}^{+1} \frac{GPDs\ (x,\xi,t)}{x \pm \xi + i\varepsilon} dx + \ldots \sim \quad P\int_{-1}^{+1} \frac{GPDs\ (x,\xi,t)}{x \pm \xi} dx \pm i\pi GPDs\ (\pm\xi,\xi,t) + \ldots$$

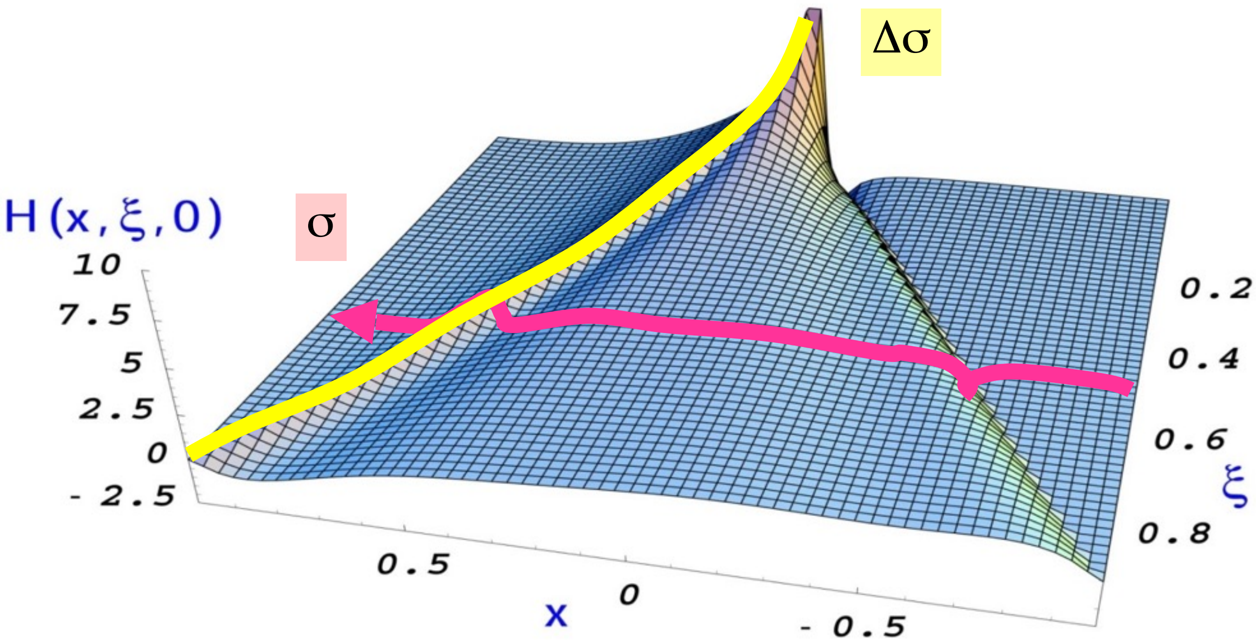

Only ξ and *t* are accessible experimentally!

To get information on *x* need extensive measurements in Q^2.

Need measurements off proton and neutron to get flavour separation of CFFs in DVCS.

Which DVCS experiment?

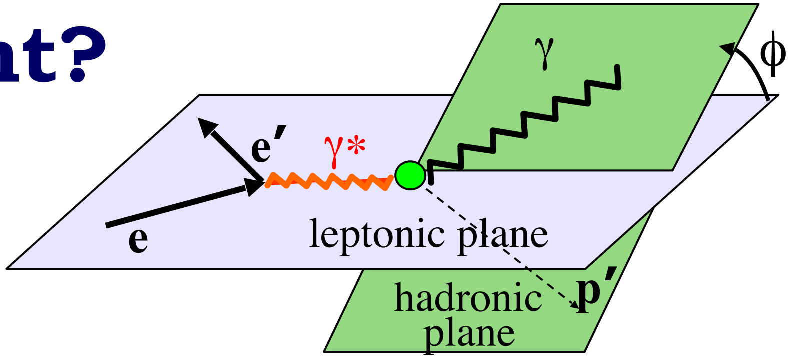

Real parts of CFFs accessible in cross-sections and double polarisation asymmetries,

imaginary parts of CFFs in single-spin asymmetries.

Beam, target polarisation

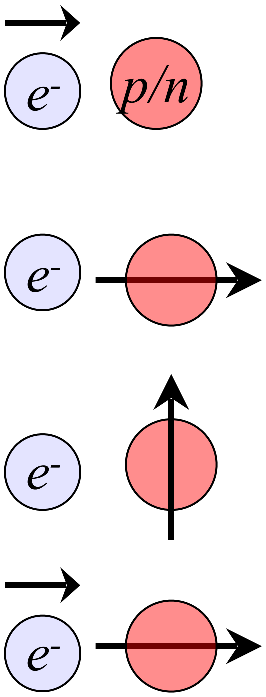

		Proton Neutron
$\Delta\sigma_{LU} \sim \sin\phi\, \Im(F_1 H + \xi G_M \tilde{H} - \frac{t}{4M^2} F_2 E)\, d\phi$	→	$Im\{\boldsymbol{H_p}, \tilde{H}_p, E_p\}$ $Im\{H_n, \tilde{H}_n, \boldsymbol{E_n}\}$
$\Delta\sigma_{UL} \sim \sin\phi\, \Im(F_1 \tilde{H} + \xi G_M (H + \frac{x_B}{2} E) - \xi \frac{t}{4M^2} F_2 \tilde{E} + \ldots)\, d\phi$	→	$Im\{\boldsymbol{H_p}, \boldsymbol{\tilde{H}_p}\}$ $Im\{\boldsymbol{H_n}, E_n, \tilde{E}_n\}$
$\Delta\sigma_{UT} \sim \cos\phi\, \Im(\frac{t}{4M^2}(F_2 H - F_1 E) + \ldots) d\phi$	→	$Im\{\boldsymbol{H_p}, \boldsymbol{E_p}\}$ $Im\{\boldsymbol{H_n}\}$
$\Delta\sigma_{LL} \sim (A + B\cos\phi)\, \Re(F_1 \tilde{H} + \xi G_M (H + \frac{x_B}{2} E) + \ldots) d\phi$	→	$Re\{\boldsymbol{H_p}, \boldsymbol{\tilde{H}_p}\}$ $Re\{\boldsymbol{H_n}, E_n, \tilde{E}_n\}$

Jefferson Lab

JLab: 6 GeV era

CEBAF: Continuous Electron Beam Accelerator Facility.

- Energy up to ~6 GeV
- Energy resolution: $\delta E / E_e \sim 10^{-5}$
- Longitudinal electron polarisation up to ~85%

Hall B: CLAS

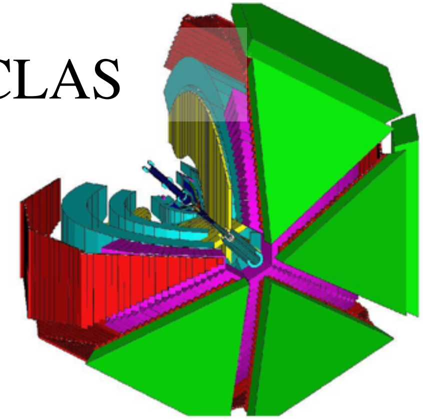

- Very large acceptance detector array for multi-particle final states.

12 GeV era

- Maximum electron energy: 12 GeV to new Hall D
- 11 GeV deliverable to Halls A, B and C

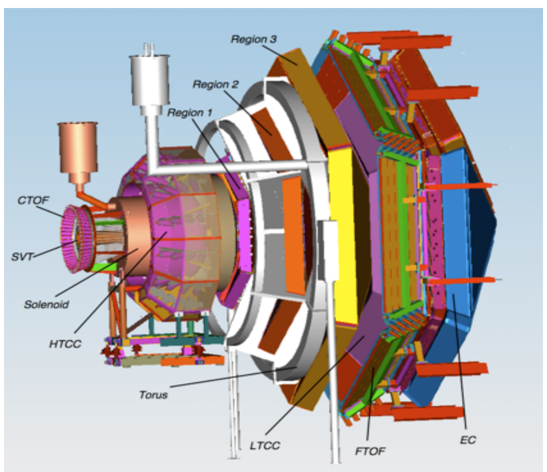

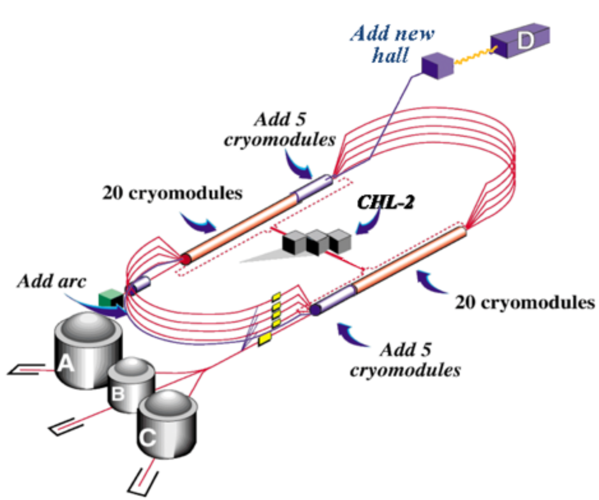

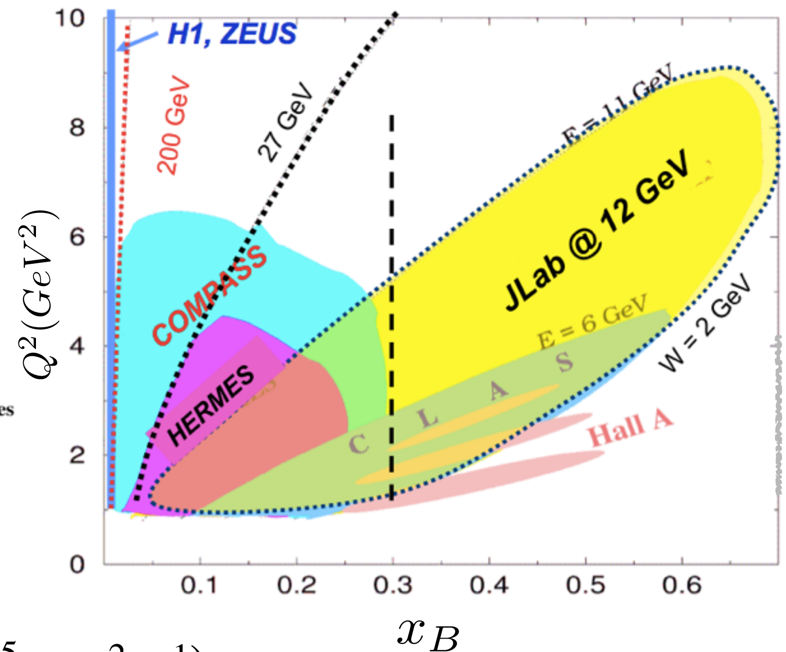

CLAS12: Very large acceptance, high luminosity (~10^{35} cm^{-2} s^{-1})

CLAS12

Design luminosity

$L \sim 10^{35}$ cm^{-2} s^{-1}

High luminosity & large acceptance:

Concurrent measurement of exclusive, semi-inclusive, and inclusive processes

Acceptance for photons and electrons:

- $2.5^o < \theta < 125^o$

Acceptance for all charged particles:

- $5^o < \theta < 125^o$

Acceptance for neutrons:

- $5^o < \theta < 120^o$

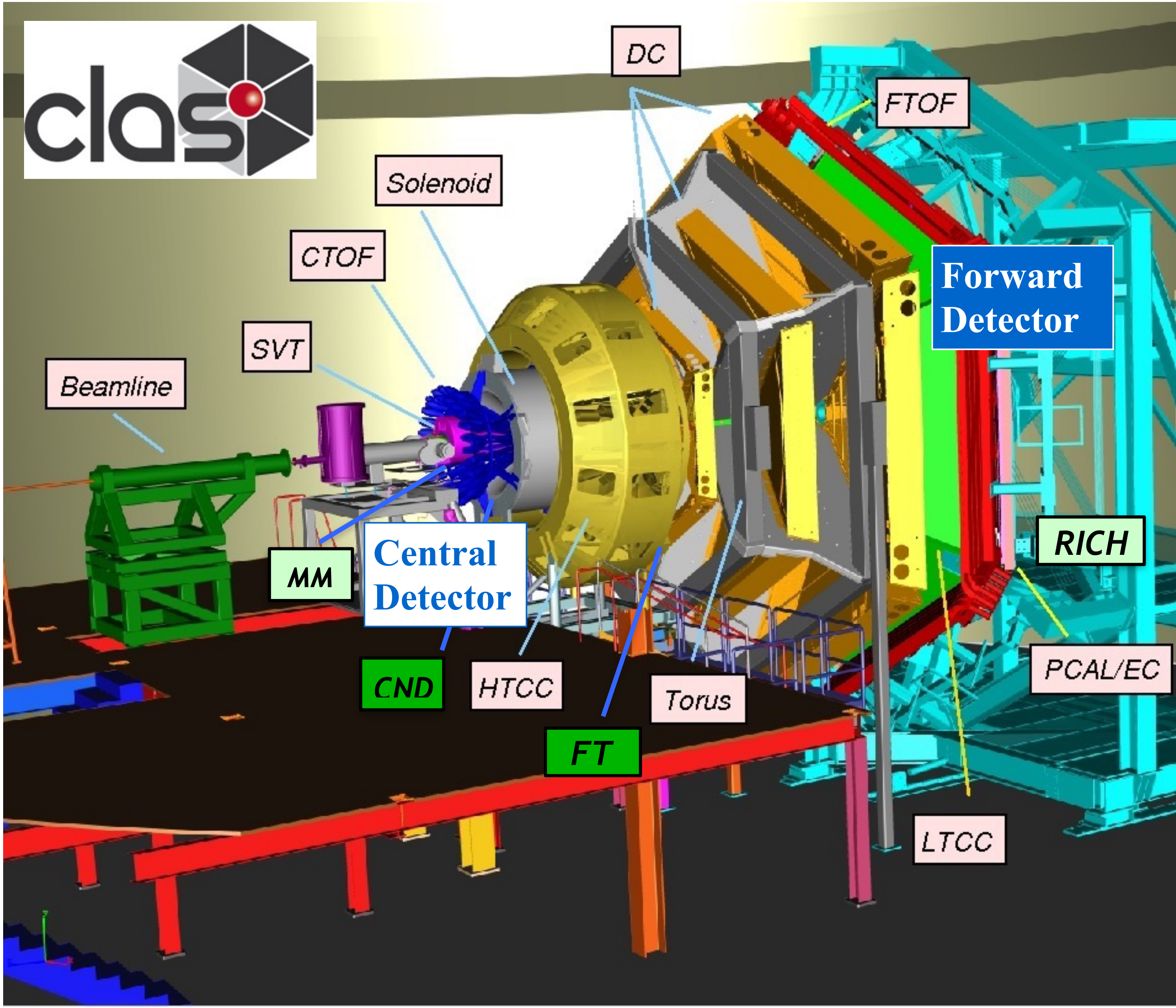

DVCS in Hall A @ 11 GeV

Detect electron in the Left High Resolution Spectrometer (HRS-L): 0.01% momentum resolution

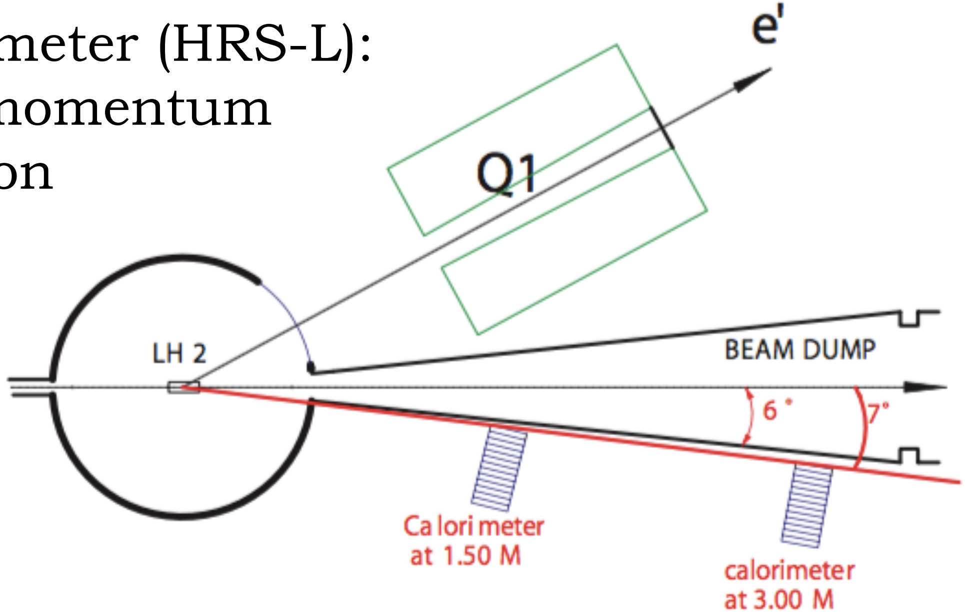

Detect photon in PbF_2 calorimeter: < 3% energy resolution

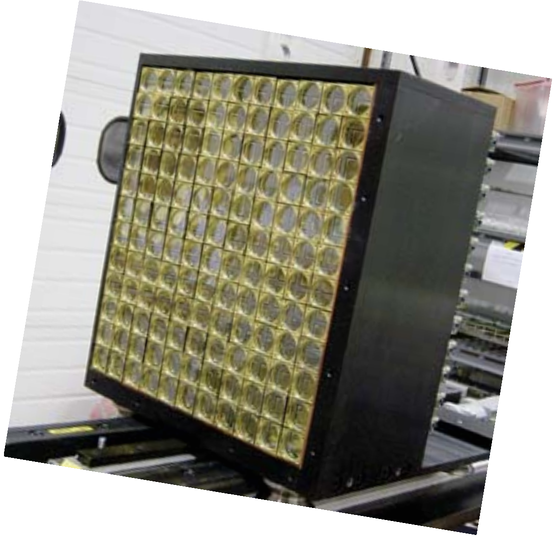

Reconstruct recoiling proton through missing mass.

DVCS in Hall C @ 11 GeV

Detect electron with (Super) High Momentum Spectrometer, (S)HMS.

Detect photon in $PbWO_4$ calorimeter.

Sweeping magnet to reduce backgrounds in calorimeter.

Reconstruct recoiling proton through missing mass.

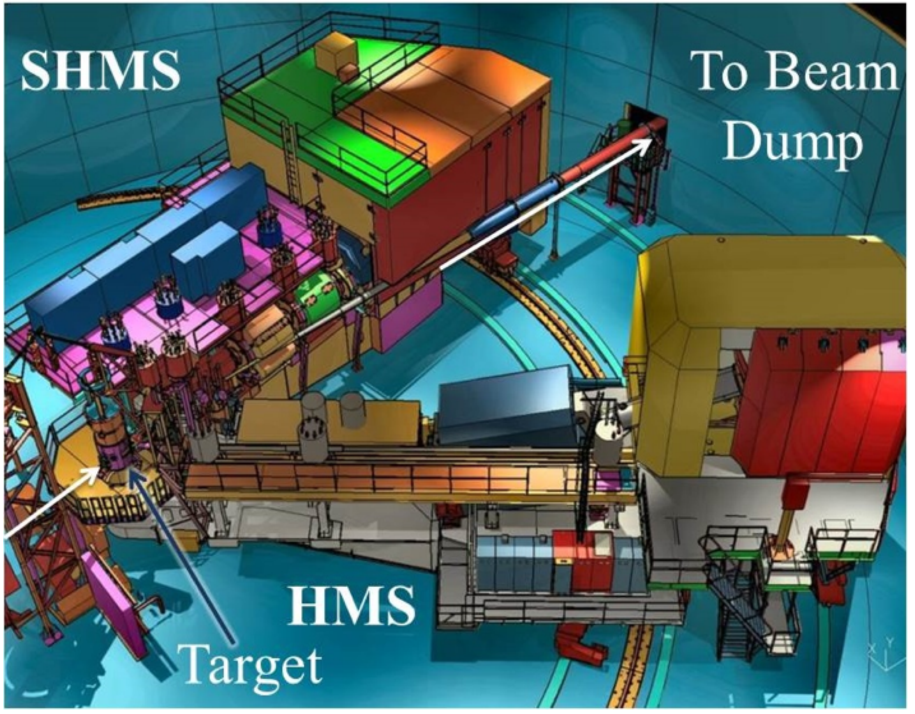

DVCS @ JLab
6 GeV era

Hall A

First DVCS cross-sections in valence region

- Hall A, ran in 2004, high precision, narrow kinematic range. Data recently re-analysed. Q^2: 1.5 - 2.3 GeV^2, $x_B = 0.36$.

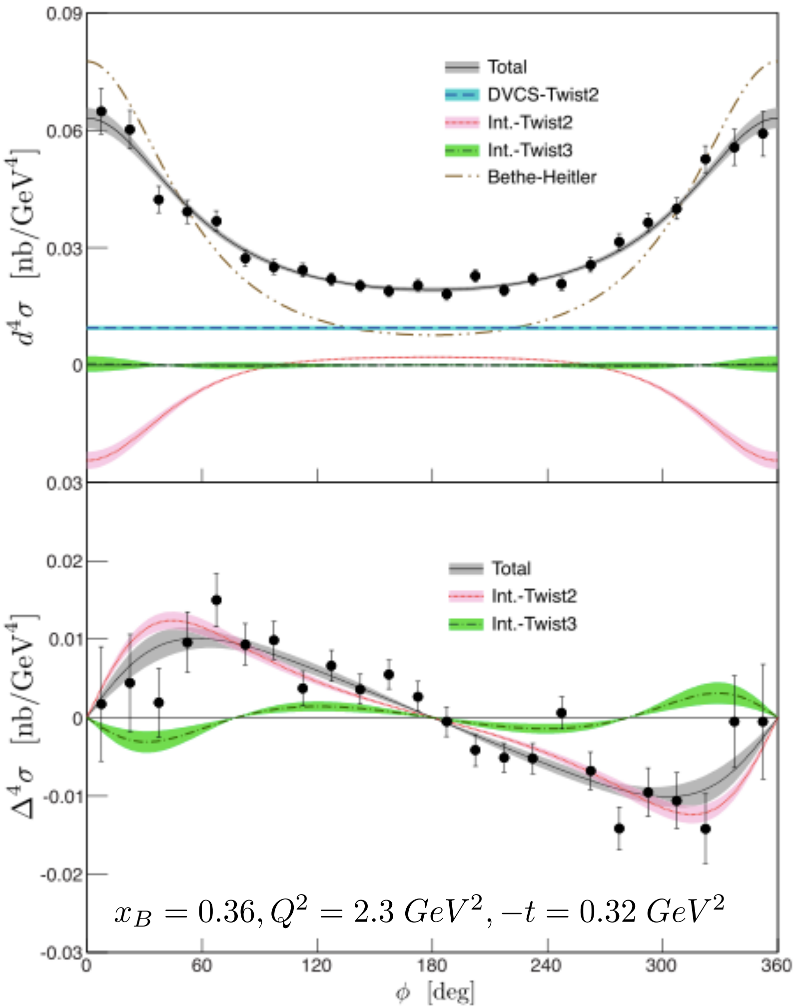

- CFFs show scaling in DVCS: leading twist (twist-2) dominance at moderate Q^2 (1.5 - 2.3 GeV^2).
- GPDs can be extracted at JLab kinematics.
- Extraction of $|T_{DVCS}|^2$ amplitude as well as interference terms is possible.

↓

- Strong deviation of DVCS cross-section from BH: new experiment to $|T_{DVCS}|^2$s energy dependence and isolate .
  E07-007, C. Muñoz *et al*.

M. Defurne *et al*, ***PRC* 92** (2015) 055202.

Hall A

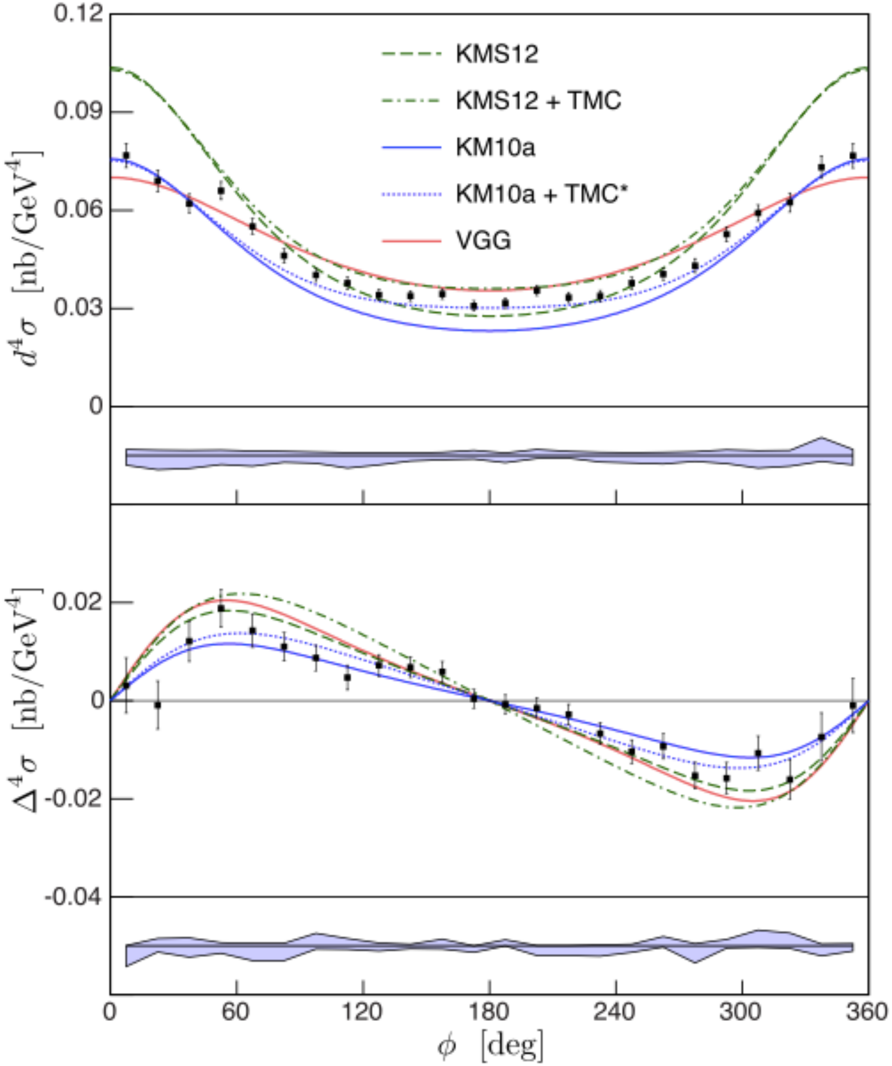

$x_B = 0.36, Q^2 = 1.9\ GeV^2, -t = 0.32\ GeV^2$

First DVCS cross-sections in valence region

- KMS parameters tuned on very low x_B meson-production data
- Target-mass and finite-t corrections (TMC) improve agreement for KM10a model

VGG model: Vanderhaeghen, Guichon, Guidal

KMS model: Kroll, Moutarde, Sabatié

KM model: Kumericki, Mueller

M. Defurne *et al*, ***PRC* 92** (2015) 055202.

Hall A DVCS cross-sections at different beam energies

- E07-007: Hall A experiment to measure helicity-dependent and -independent cross-sections at two beam energies and constant x_B, Q^2 and t.

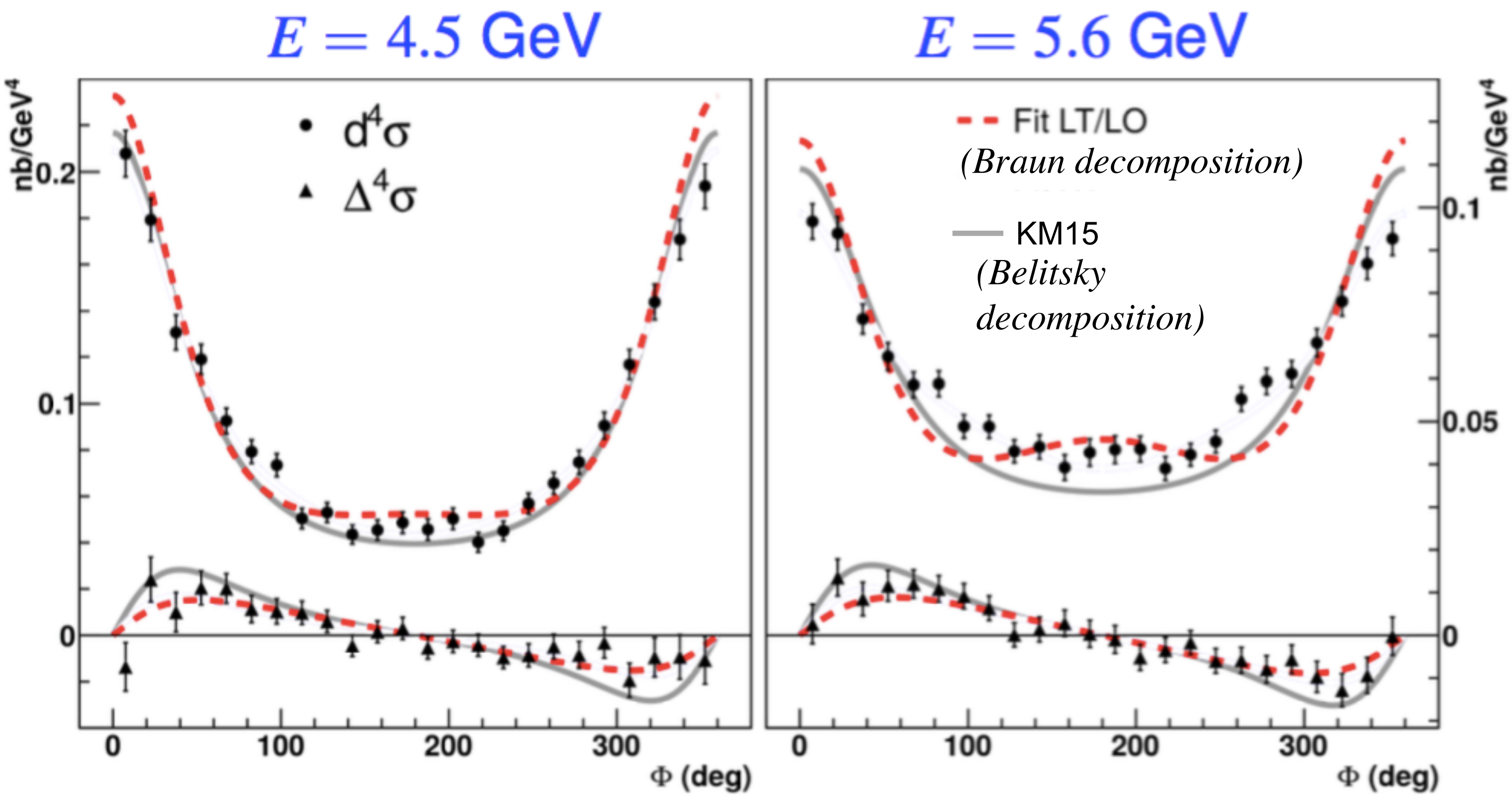

- Using the Braun decomposition, a simultaneous fit to cross-sections at both energies using only leading twist and leading order (LT/LO) does not describe the cross-sections fully: higher twist/order effects!

M. Defurne *et al*, arXiv:1703.09442 V. Braun *et al*, ***PRD 89*** (2014) 074022.

Hall A

DVCS cross-sections at different beam energies

* Including either higher order or higher twist effects (HT) improves the match with data:

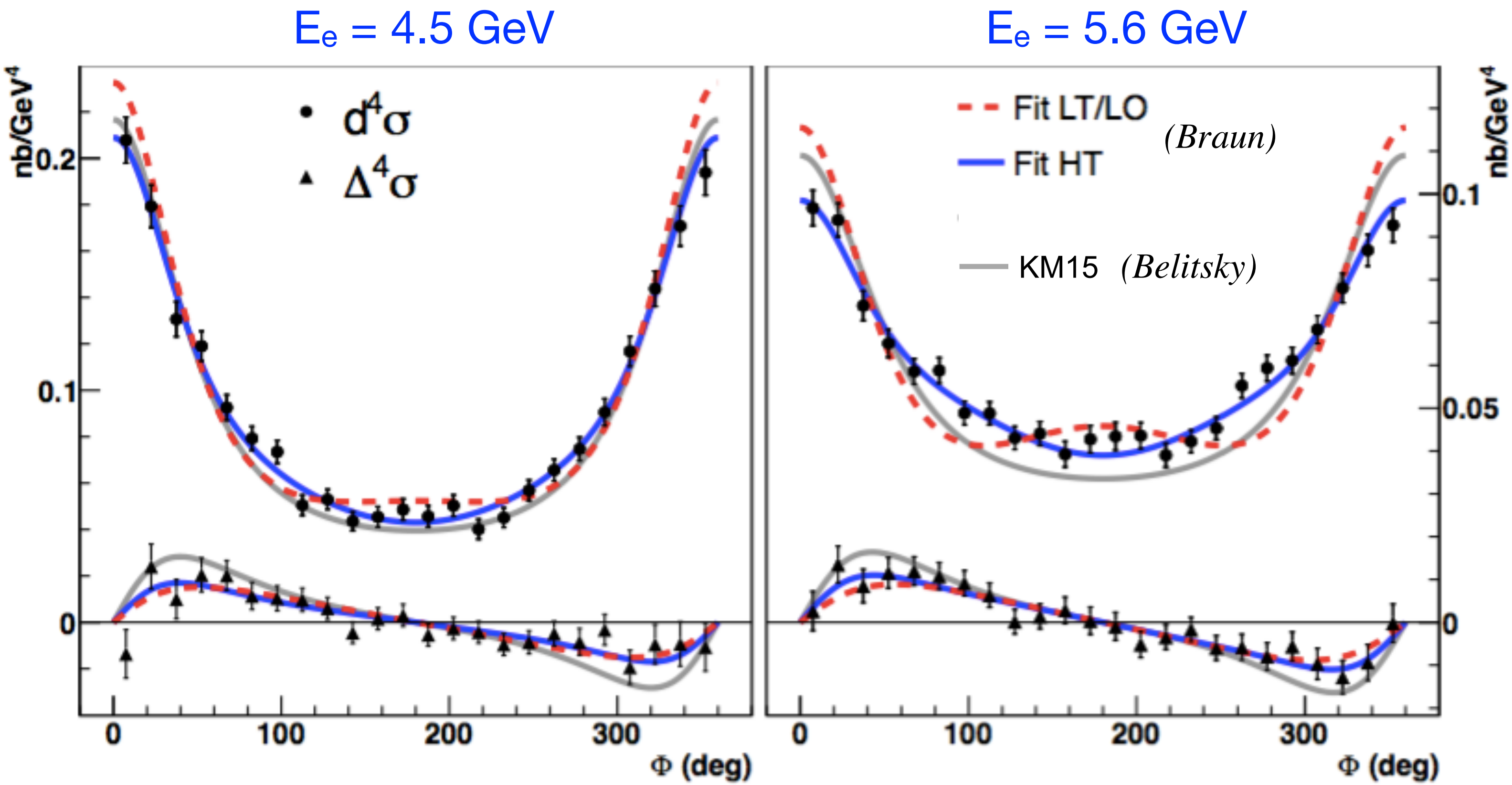

Higher-order and / or higher-twist terms are important!

More data necessary to determine between them.

M. Defurne *et al*, arXiv:1703.09442

CLAS unpolarised cross-sections

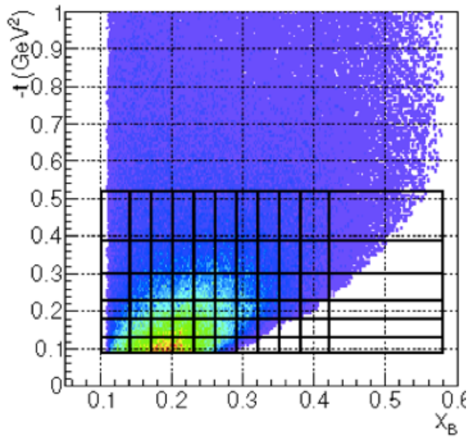

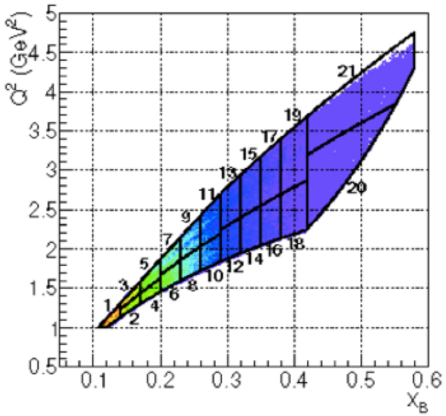

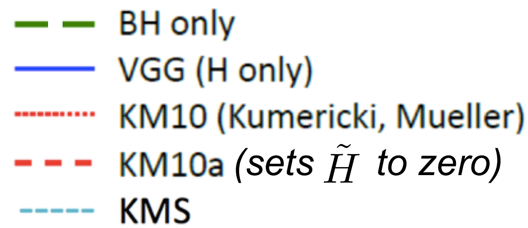

$$\frac{d^4\sigma_{ep\to ep\gamma}}{dQ^2 dx_B dt d\Phi}$$

$$\frac{1}{2}\left(\frac{d^4\overrightarrow{\sigma}_{ep\to ep\gamma}}{dQ^2 dx_B dt d\Phi} - \frac{d^4\overleftarrow{\sigma}_{ep\to ep\gamma}}{dQ^2 dx_B dt d\Phi}\right)$$

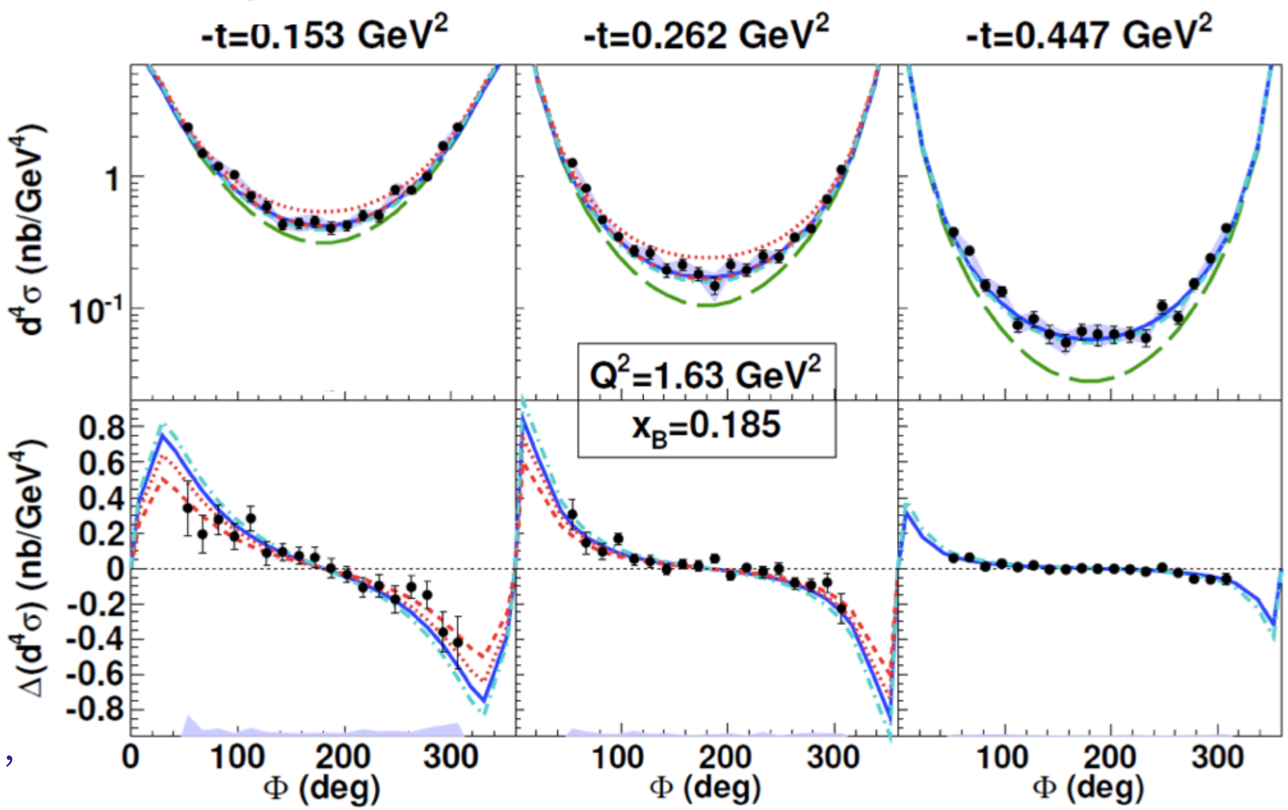

H.-S. Jo *et al* (CLAS Collaboration), ***PRL*** **115** (2015) 212003

Beam- and target-spin asymmetries

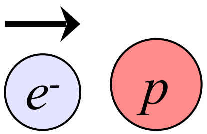

A_{LU} (BSA) characterised by imaginary parts of CFFs via:

$$F_1 H + \xi G_M \tilde{H} - \frac{t}{4M^2} E$$

- Pioneering measurement at CLAS: S. Stepanyan *et al* (CLAS), ***PRL* 87** (2001) 182002
- First high-statistics measurement in extended kinematics, qualitative agreement with leading models, constraints on fit parameters for the extraction of CFFs: F.-X. Girod *et al* (CLAS), ***PRL* 100** (2008) 162002

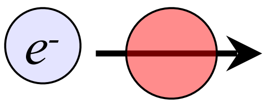

A_{UL} (lTSA) characterised by imaginary parts of CFFs via:

$$F_1 \tilde{H} + \xi G_M (H + \frac{x_B}{2} E) - \frac{\xi t}{4M^2} F_2 \tilde{E} + ...$$

- First measurement at CLAS: S. Chen *et al* (CLAS), ***PRL* 97** (2006) 072002
- High statistics, large kinematic coverage, strong constraints on fits, simultaneous fit with BSA and double-spin asymmetry (DSA) from the same dataset.

E. Seder *et al* (CLAS), ***PRL* 114** (2015) 032001
S. Pisano *et al* (CLAS), ***PRD* 91** (2015) 052014

Single experiment with longitudinally polarised NH_3 target, allowed simultaneous extraction of BSA, TSA and DSA at common kinematics.

Beam- and target-spin asymmetries

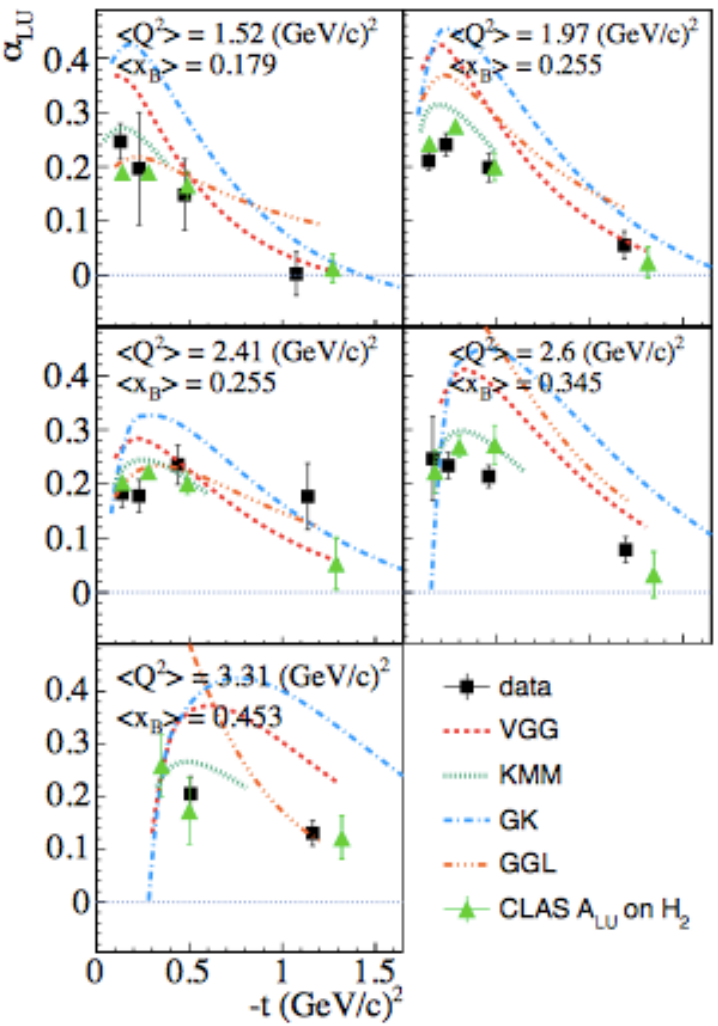

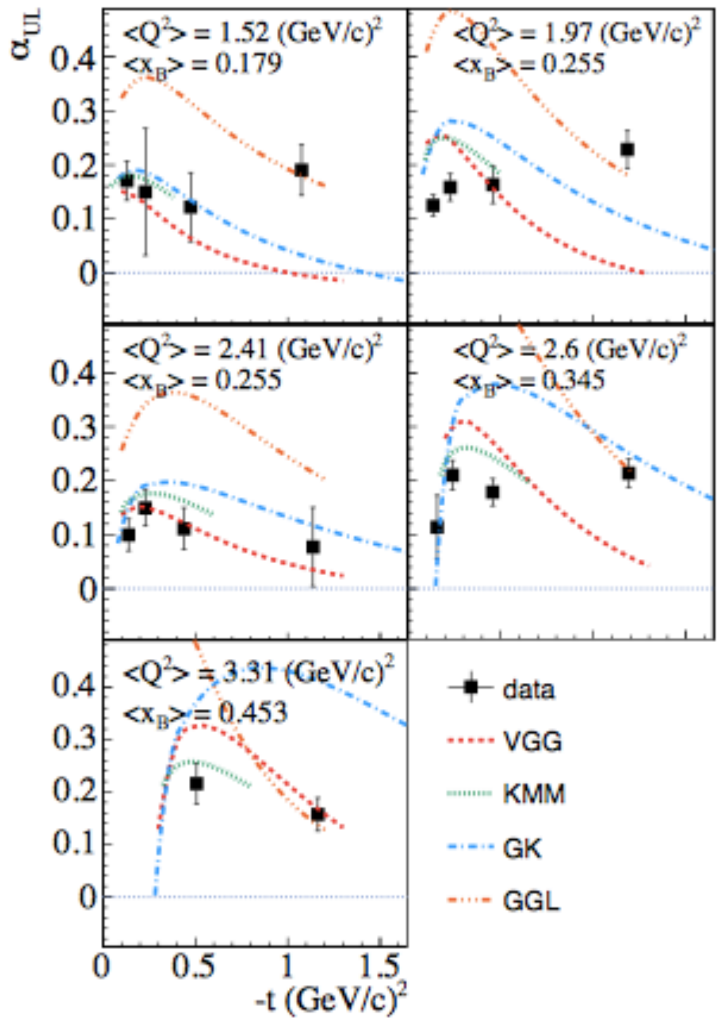

$$A = \frac{\alpha sin\phi}{1+\beta cos\phi}$$

GGL: Goldstein, Gonzalez, Liuti

GK: Kroll, Moutarde, Sabatié

KMM: Kumericki, Mueller, Murray

S. Pisano *et al* (CLAS Collaboration), ***PRD*** **91** (2015) 052014

E. Seder *et al* (CLAS Collaboration), ***PRL*** **114** (2015) 032001

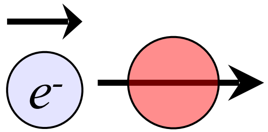

Double-spin Asymmetry (A_{LL})

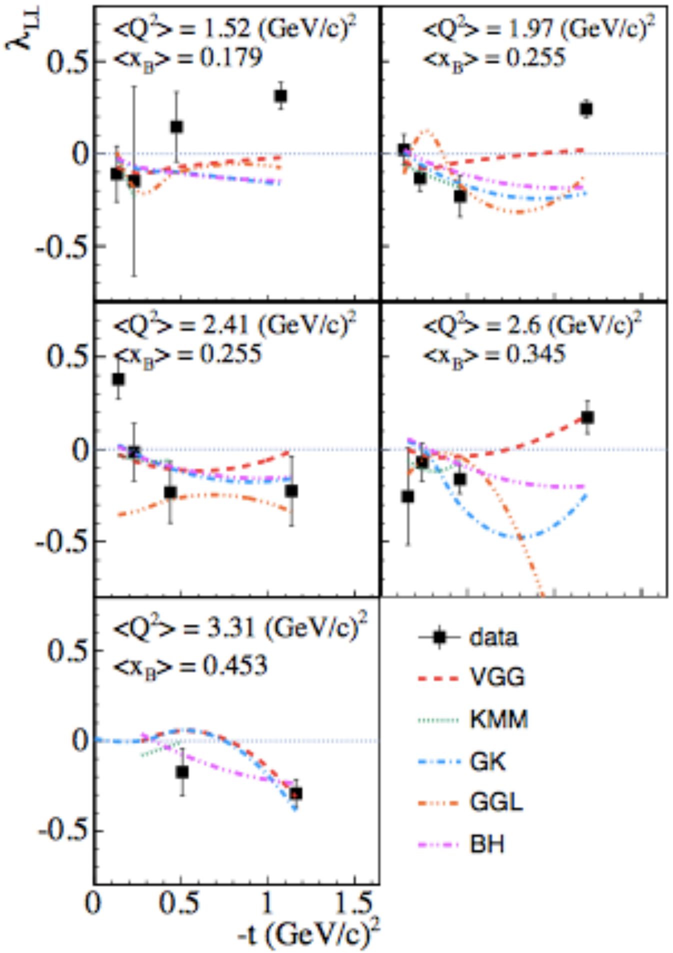

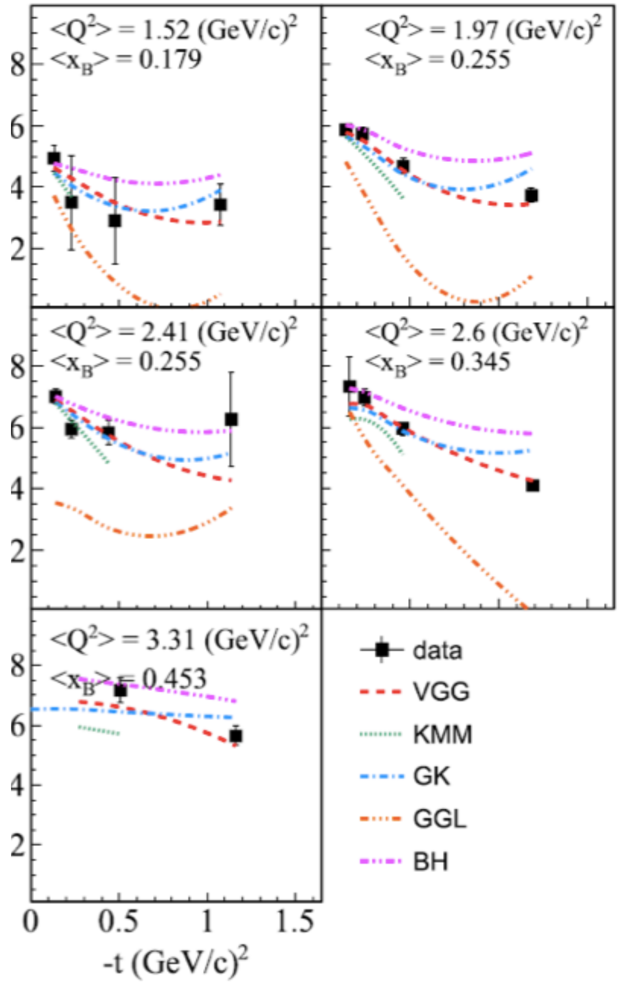

A_{LL} from fit to asymmetry:

$$\frac{\kappa_{LL} + \lambda_{LL}\cos\phi}{1 + \beta\cos\phi}$$

A_{LL} characterised by real parts of CFFs via:

$$F_1 \tilde{H} + \xi G_M (H + \frac{x_B}{2} E) + \ldots$$

- Fit parameters extracted from a simultaneous fit to BSA, TSA and DSA.
- CFF extraction from three spin asymmetries at common kinematics.

E. Seder *et al* (CLAS Collaboration), ***PRL* 114** (2015) 032001
S. Pisano *et al* (CLAS Collaboration), ***PRD* 91** (2015) 052014

What can we learn from the asymmetries?

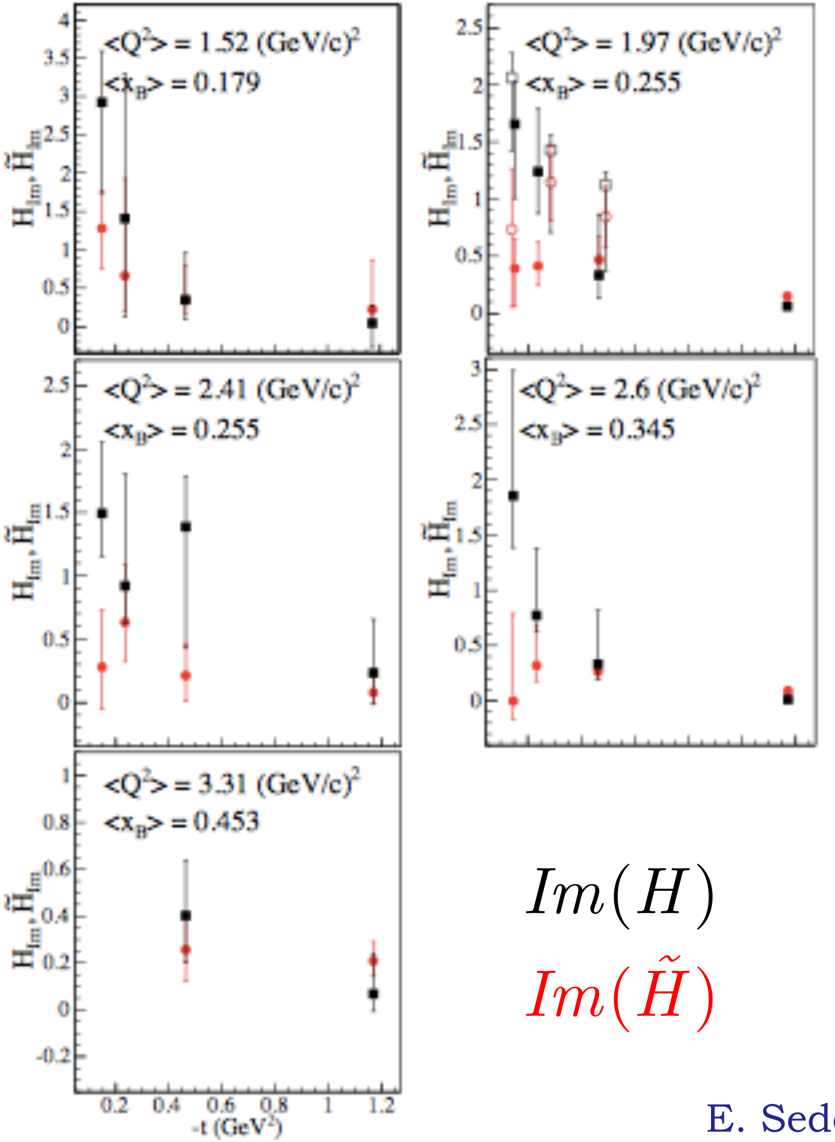

$Im(H)$

$Im(\tilde{H})$

Answers hinge on a global analysis of all available data.

$$H^q(x,0,0) = f_1(x)$$

$$\tilde{H}^q(x,0,0) = g_1(x)$$

Information on relative distributions of quark momenta (PDFs) and quark helicity, $\Delta q(x)$.

Indications that axial charge is more concentrated than electromagnetic charge

E. Seder *et al* (CLAS Collaboration), ***PRL* 114** (2015) 032001
S. Pisano *et al* (CLAS Collaboration), ***PRD* 91** (2015) 052014

Towards a tomographic image of the proton

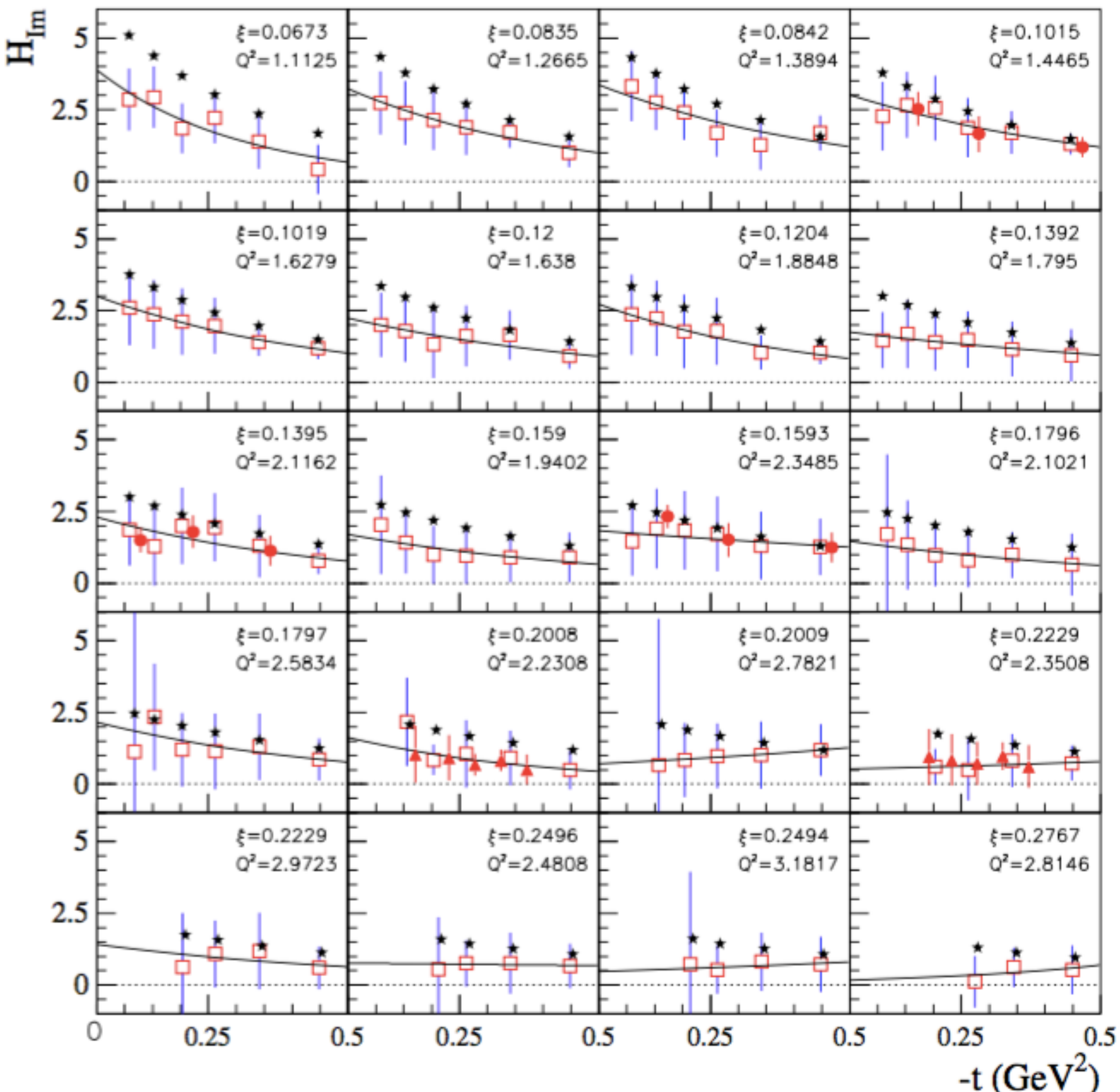

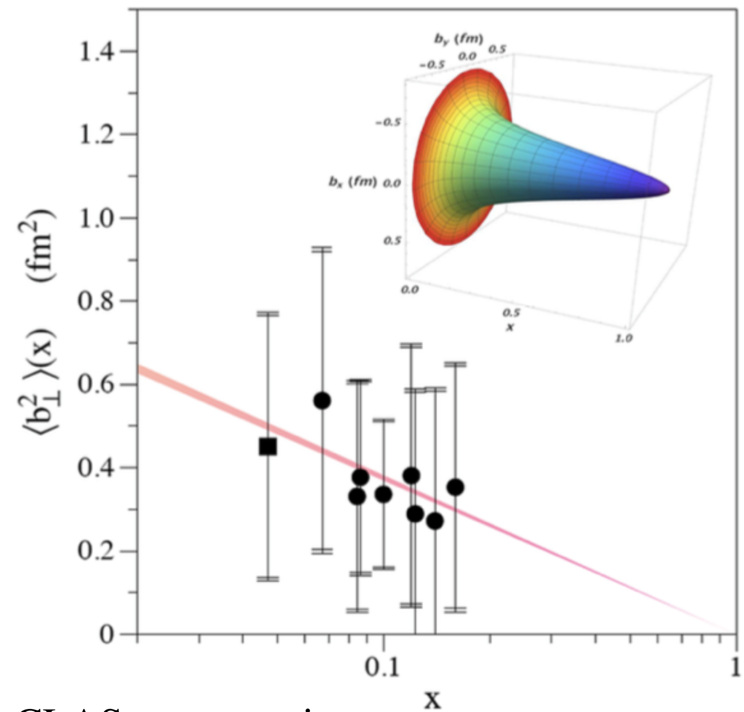

- □ CLAS cross-sections
- — Ae^{bt} exponential fit to the above
- ▲ Hall A cross-sections
- ● CLAS cross-sections, TSA and DSA
- ★ VGG reference CFFs

Slope in t becomes flatter at higher ξ:

valence quarks at centre, sea quarks at the periphery.

Dupré, Guidal, Vanderhaeghen, PRD95, 011501(R) (2017)

Future DVCS with Lab @ 12 GeV

DVCS Cross-sections: Halls A and C

Experiments:
E12-06-114 (Hall A, 100 days),
E12-13-010 (Hall C, 53 days)
C. Muñoz Camacho et al.,
C. Hyde et al.

Unpolarised liquid H_2 target:

- Beam energies: 6.6, 8.8, 11 GeV
- Scans of Q^2 at fixed x_B.
- Hall A: aim for absolute cross-sections with 4% relative precision.

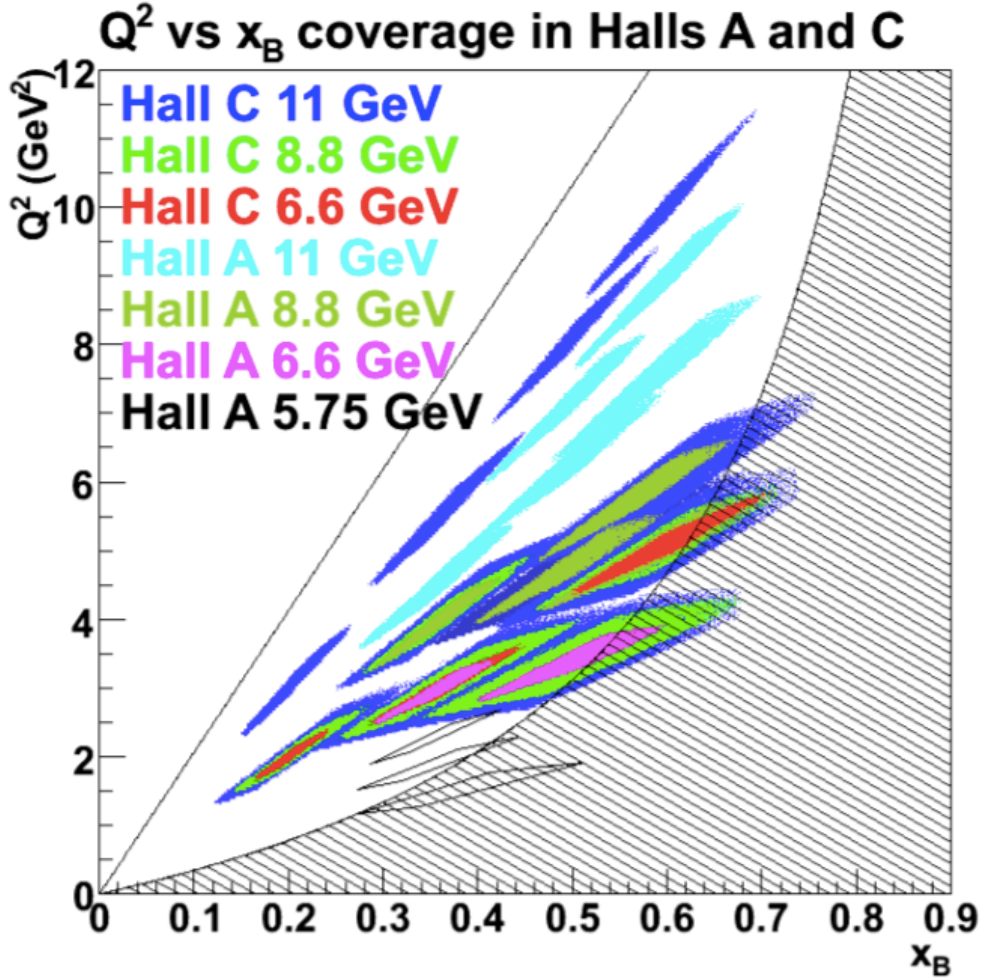

Hall A started taking data last spring!

✱ Azimuthal, energy and helicity dependencies of cross-section to separate $|T_{DVCS}|^2$ and interference contributions in a wide kinematic coverage.

✱ Separate *Re* and *Im* parts of the DVCS amplitude.

Proton DVCS @ 11 GeV

CLAS12

Experiment E12-06-119

F. Sabatié et al.

P_{beam} = 85%
L = 10^{35} $cm^{-2}s^{-1}$
1< Q^2 < 10 GeV^2
0.1 < x_B < 0.65
$-t_{min} < -t < 2.5$ GeV^2

Kinematics similar for all proton DVCS @ 11 GeV with CLAS12 experiments

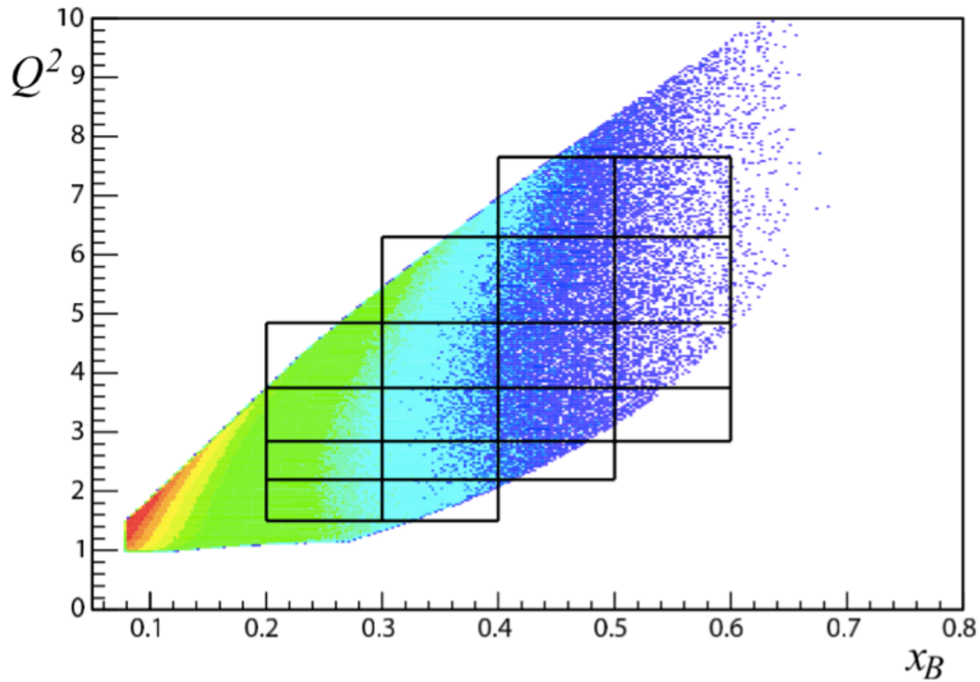

First experiment with CLAS12!

Unpolarised liquid H_2 target:

- Statistical error: 1% - 10% on sinφ moments
- Systematic uncertainties: ~ 6 - 8%

Due to start this autumn!

A_{LU} characterised by imaginary parts of CFFs via:

$$F_1 H + \xi G_M \tilde{H} - \frac{t}{4M^2} E \longrightarrow \textit{Im}(H_p)$$

Proton DVCS with a longitudinally polarised target

CLAS12

Experiment E12-06-119
F. Sabatié et al.

A_{UL} characterised by imaginary parts of CFFs via: $$F_1\tilde{H} + \xi G_M(H + \frac{x_B}{2}E) - \frac{\xi t}{4M^2}F_2\tilde{E} + \ldots$$

→ $Im(\widetilde{H}_p)$

Longitudinally polarised NH_3 target:

- Dynamic Nuclear Polarisation (DNP) of target material, cooled to 1K in a *He* evaporation cryostat.
- $P_{proton} > 80\%$
- Statistical error: 2% - 15% on sinφ moments
- Systematic uncertainties: ~ 12%

Tentative schedule: 2020

Target cryostat

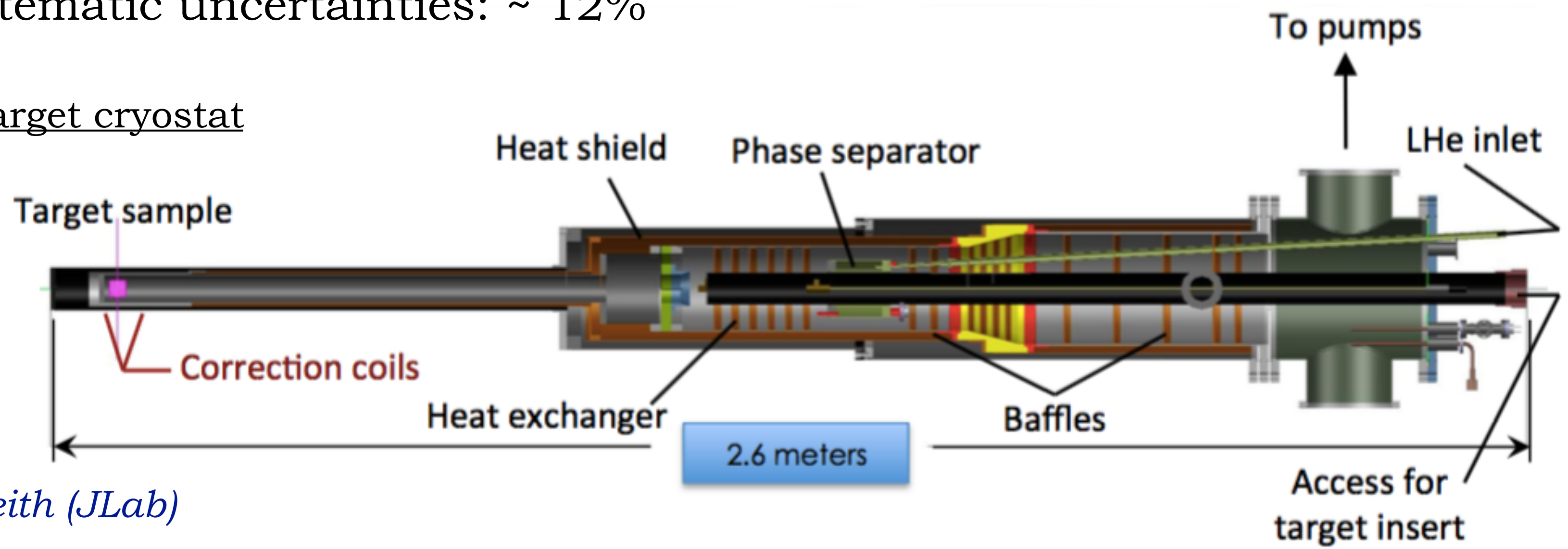

C. Keith (JLab)

Proton DVCS @ 11 GeV

CLAS12

Impact of CLAS12 unpolarised target proton-DVCS data on the extraction of Re(H) and Im(H).

Re(H)

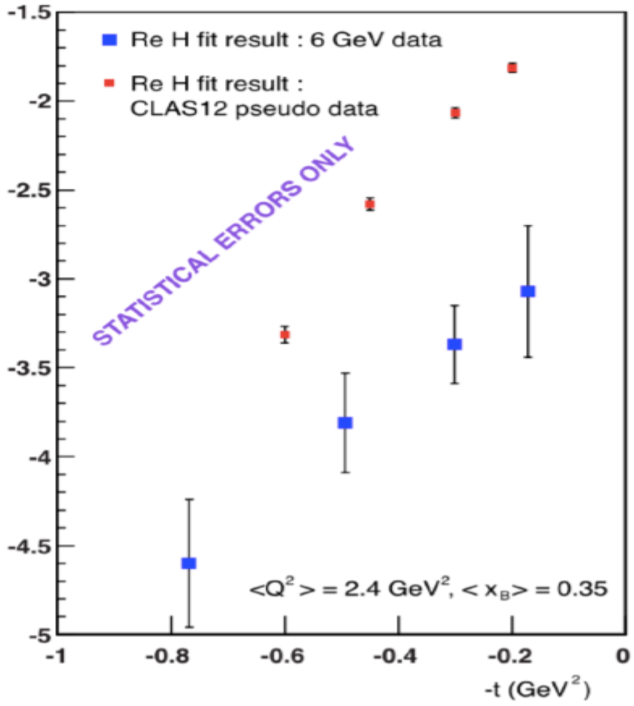

Im(H)

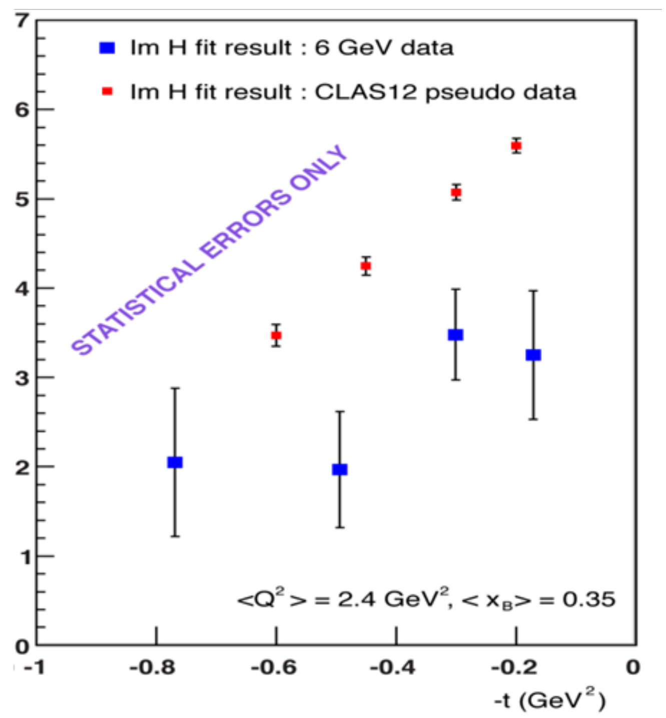

(CLAS 6 GeV extraction H. Moutarde)

DVCS at lower energies with CLAS12

CLAS12

Experiment E12-16-010B
F.-X. Girod et al.

Unpolarised liquid H_2 target:

- Beam energies: 6.6, 8.8 GeV
- Simultaneous fit to beam-spin and total cross-sections.

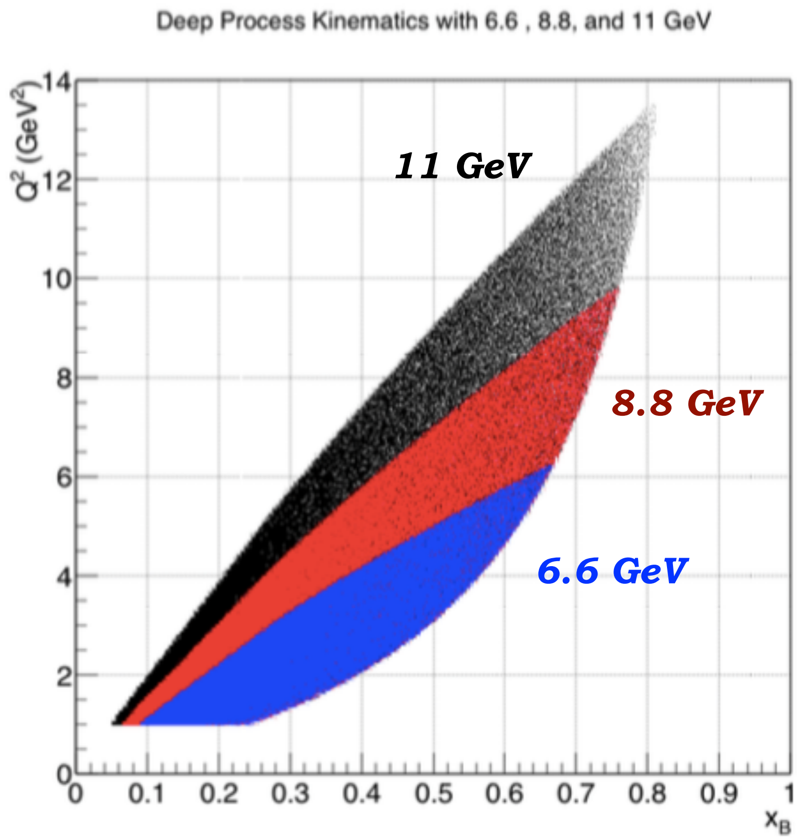

✱ Rosenbluth separation of interference and $|T_{DVCS}|^2$ terms in the cross-section

✱ Scaling tests of the extracted CFFs

✱ Model-dependent determination of the D-term in the Dispersion Relation between *Re* and *Im* parts of CFFs.

Compare with measurements from Halls A and C: cross-check model and systematic uncertainties.

DVCS at lower energies with CLAS12

Projected extraction of CFFs (red) compared to generated values (green). Three curves on the *Re(H)* show three different scenarios for the D-term.

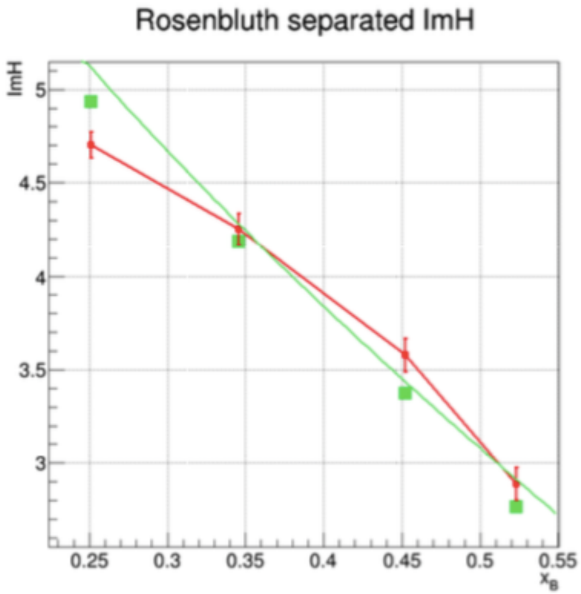

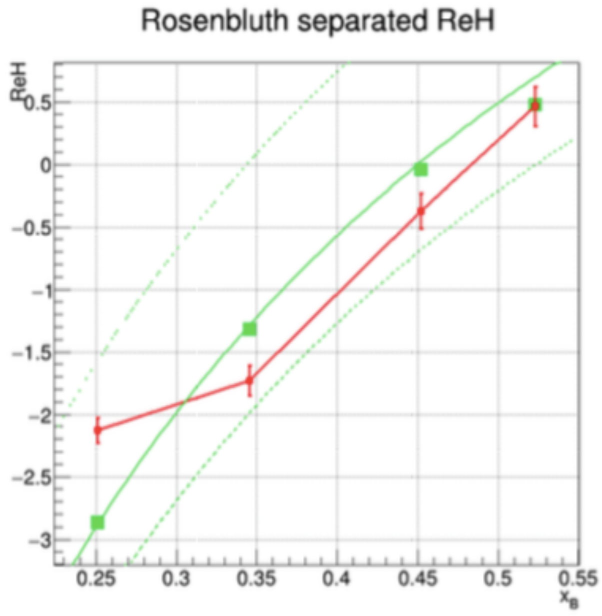

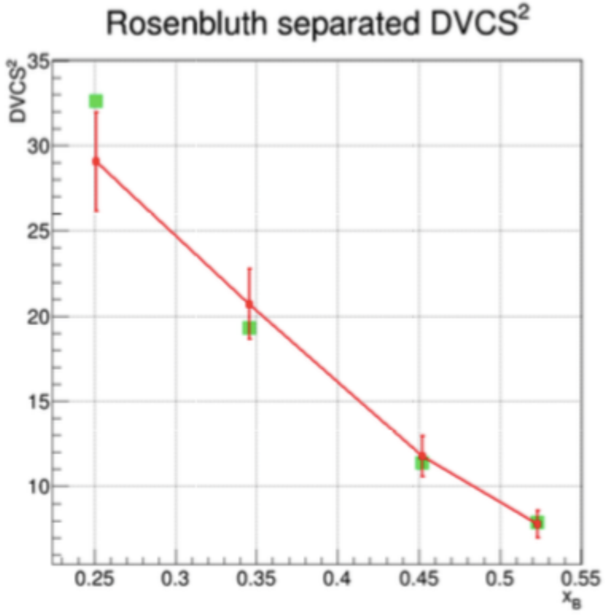

F.-X. Girod et al.

Proton DVCS with transversely polarised target at CLAS12

CLAS12

C12-12-010: with transversely polarised HD target (conditionally approved).

L. Elouardhiri et al.

$\Delta\sigma_{UT} \sim \cos\phi \; \mathrm{Im}\{k(F_2 H - F_1 E) + \ldots\ldots\} d\phi$

Sensitivity to ***Im(E)*** for the proton.

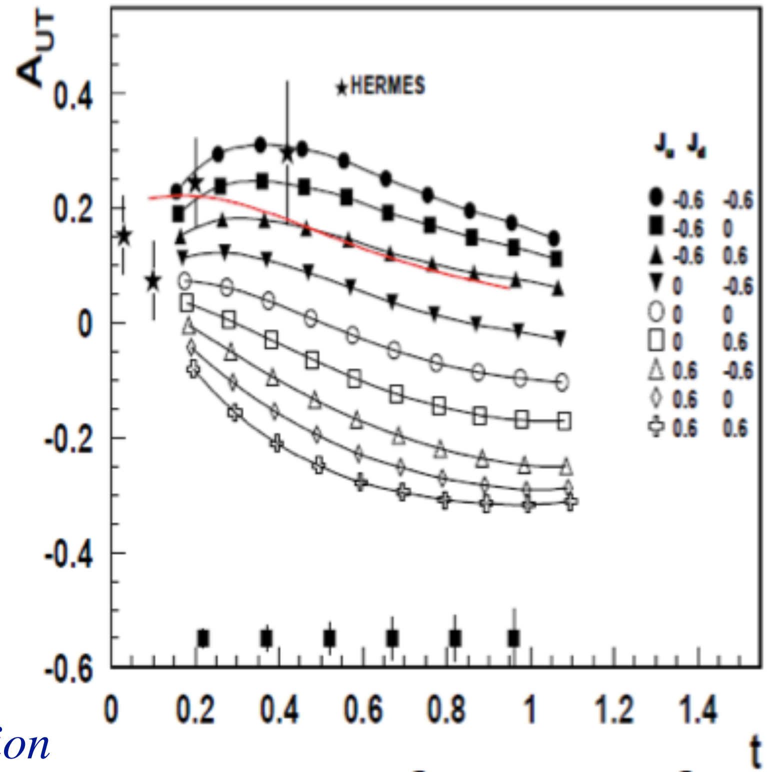

$\langle x \rangle = 0.2, \langle Q^2 \rangle = 2.5\ GeV^2$

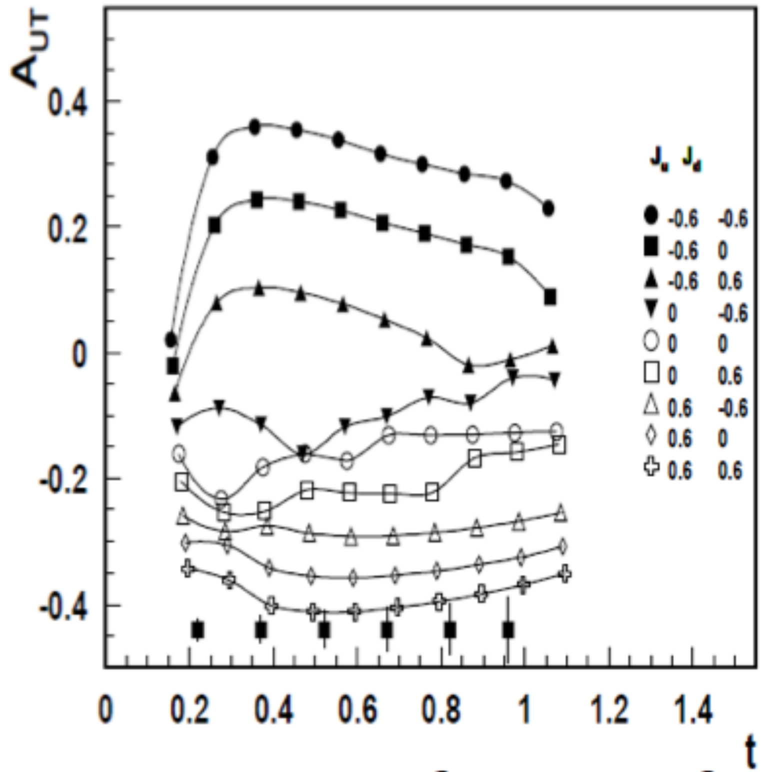

$\langle x \rangle = 0.33, \langle Q^2 \rangle = 2.5\ GeV^2$

VGG extraction (M. Guidal)

Beam-spin asymmetry in neutron DVCS @ 11 GeV

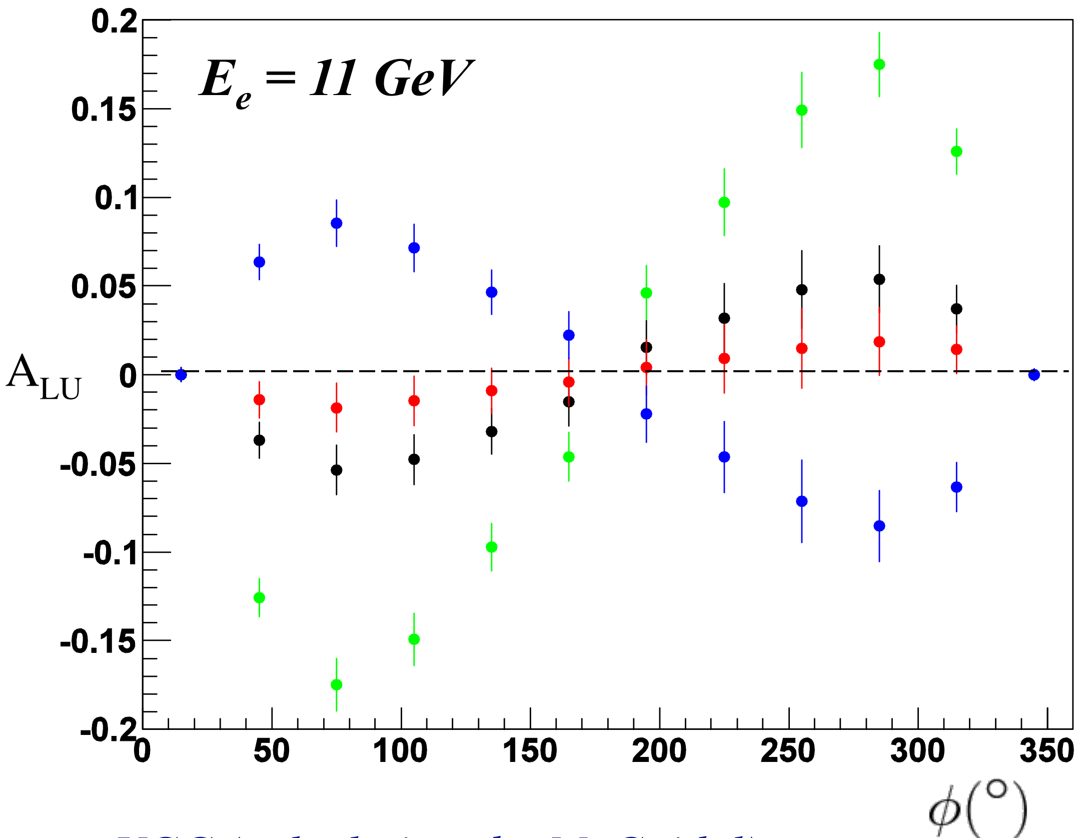

VGG (calculations by M. Guidal)

$J_u = 0.3, J_d = -0.1$ $J_u = 0.3, J_d = 0.1$

$J_u = 0.1, J_d = 0.1$ $J_u = 0.3, J_d = 0.3$

- At 11 GeV, beam spin asymmetry (A_{LU}) in neutron DVCS *is* very sensitive to J_u, J_d
- Wide coverage needed!

Fixed kinematics:

$x_B = 0.17 \quad Q^2 = 2\ \text{GeV}^2 \quad t = -0.4\ \text{GeV}^2$

First measurement of BSA in neutron-DVCS in Hall A:

M. Mazouz et al, PRL 99 (2007) 242501

Neutron DVCS @ 11 GeV

CLAS12

Experiment E12-11-003

S. Niccolai, D. Sokhan et al.

$\Delta\sigma_{LU} \sim \sin\phi\, \mathbf{Im}\{F_1 H + \xi(F_1+F_2)\tilde{H} - kF_2 E\}d\phi$

Simulated statistical sample:

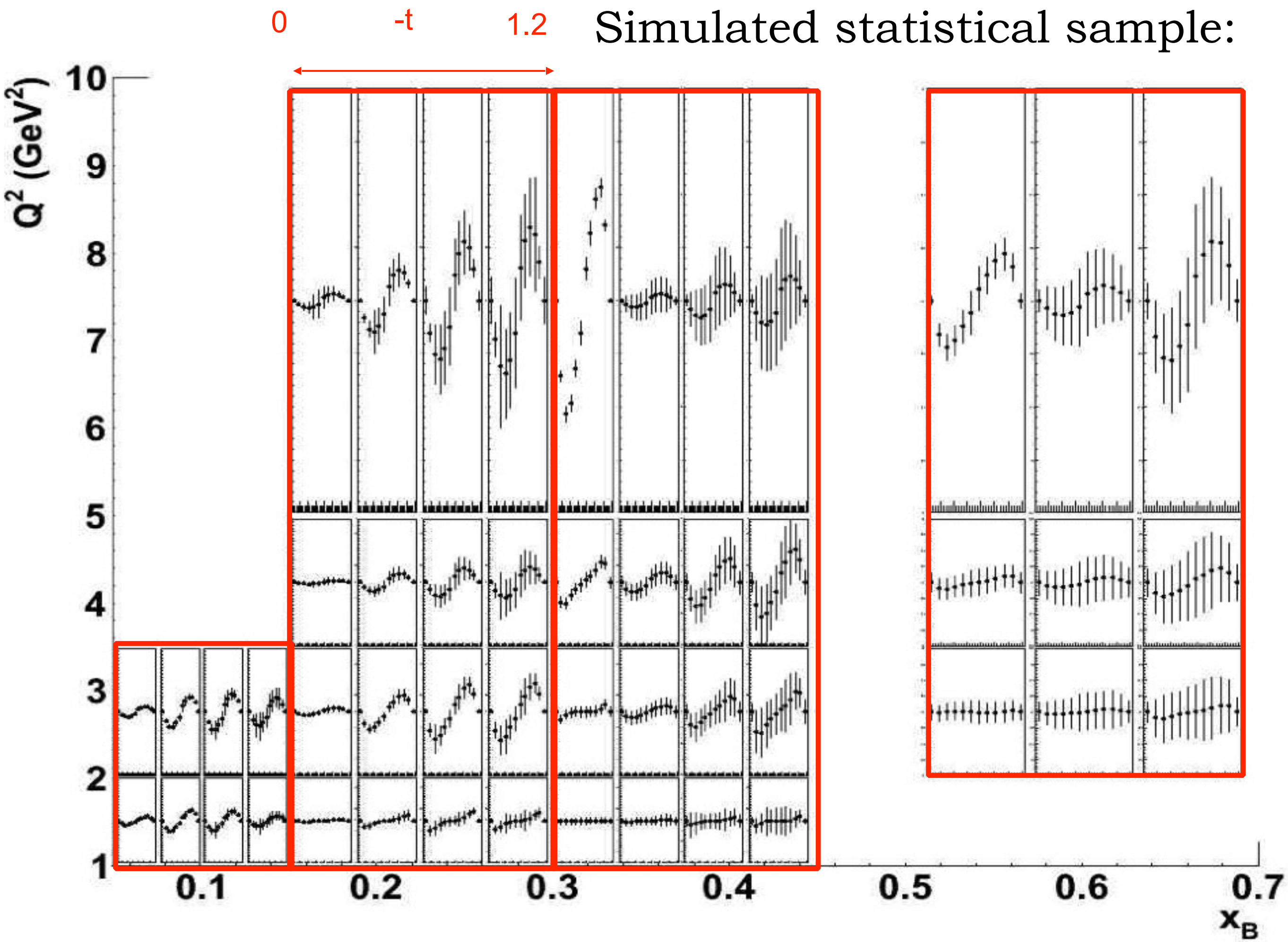

Im (E_n) dominates.

L = 10^{35} cm^{-2}s^{-1}/nucleon

$$e + d \to e' + \gamma + n + (p_s)$$

CLAS12 +
Forward Tagger +
Neutron Detector

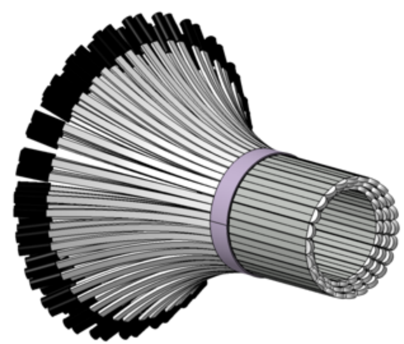

Tentative schedule: 2019

Neutron DVCS with a longitudinally polarised target

Experiment E12-06-109A.
S. Niccolai, D. Sokhan et al.

Longitudinally polarised ND_3 target:

- Dynamic Nuclear Polarisation (DNP) of target material in a cryostat shared with the NH_3 target.
- $P_{deuteron}$ up to 50%
- Systematic uncertainties: ~ 12%

A_{UL} characterised by imaginary parts of CFFs via:

$$F_1\tilde{H} + \xi G_M(H + \frac{x_B}{2}E) - \frac{\xi t}{4M^2}F_2\tilde{E} + \ldots$$

→ ***Im*(H$_n$)**

In combination with pDVCS, will allow flavour-separation of the H_q CFFs.

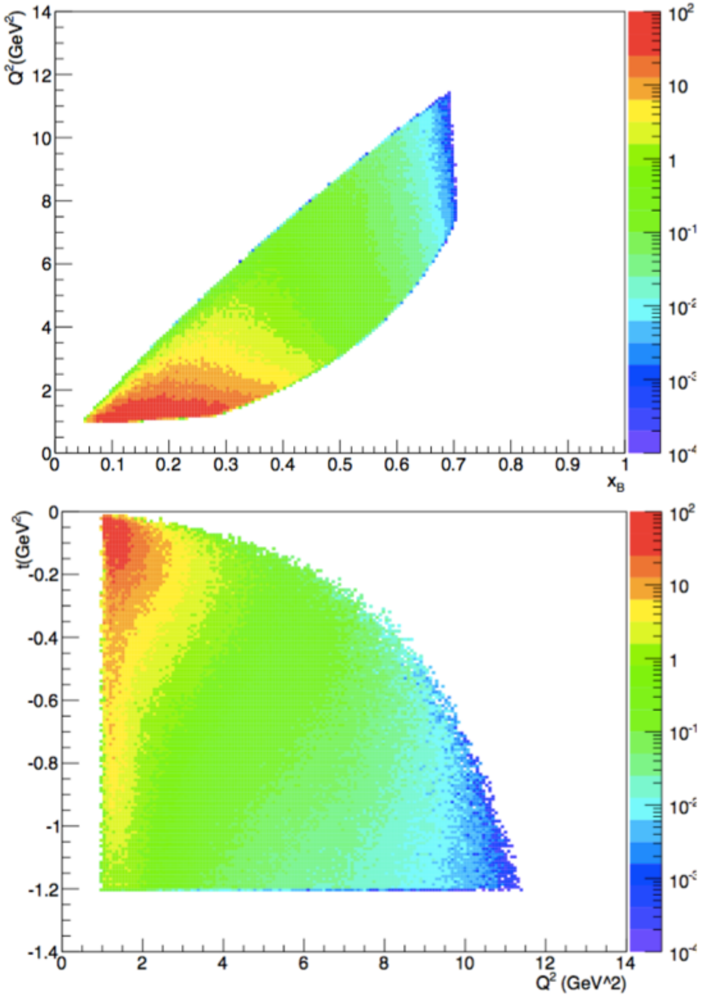

Tentative schedule: 2020

Projected sensitivities to *Im(H)* CFF

CLAS12

$Q^2 = 2.6\ GeV^2,\ x_B = 0.23$ | $Q^2 = 5.9\ GeV^2,\ x_B = 0.35$

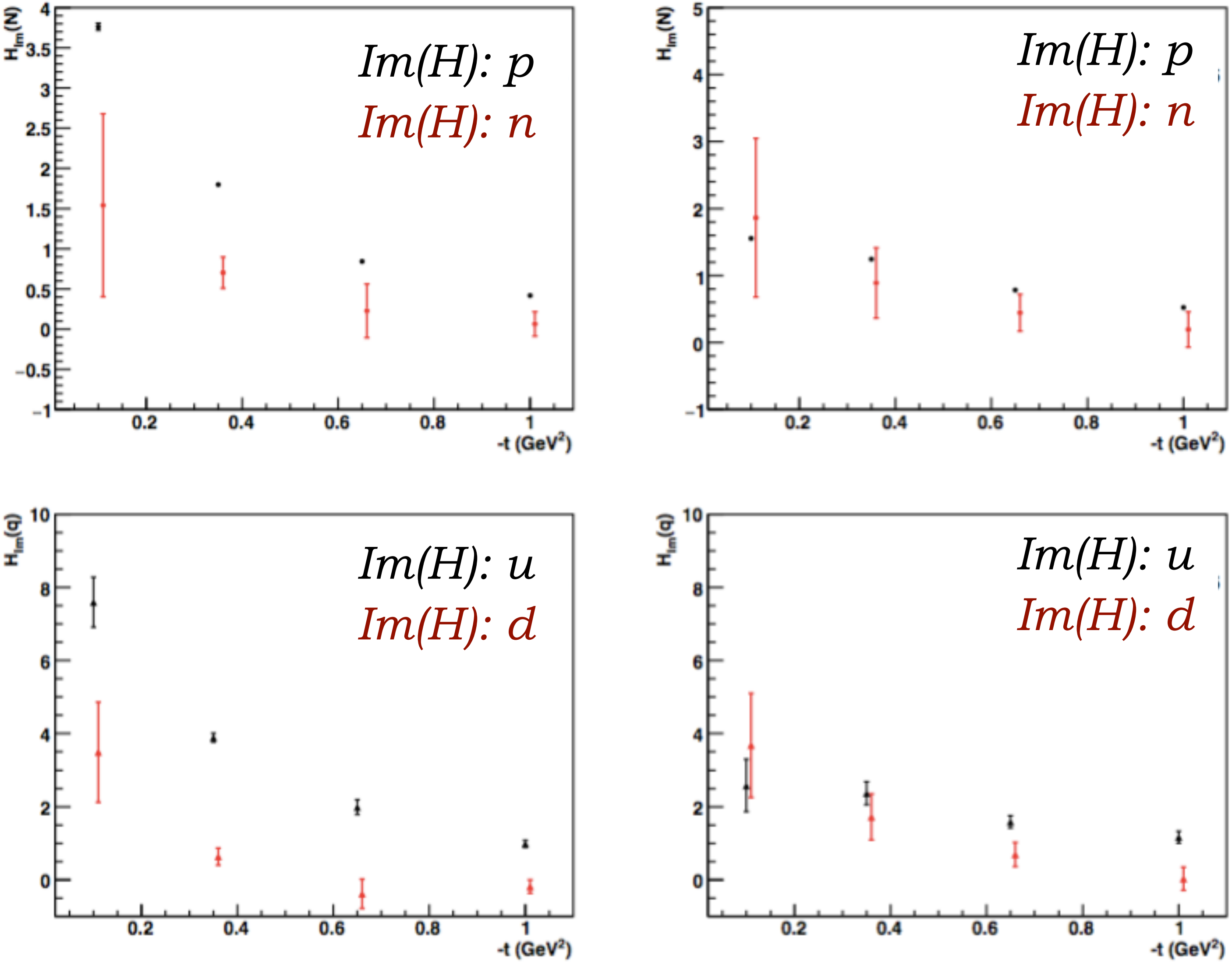

Projections for *Im(H*) neutron and proton and up and down CFFs extracted from approved CLAS12 experiments.

VGG fit (M. Guidal)

Projected sensitivities to *Im(E)* CFF

CLAS12

Q^2 = 2.6 GeV^2, x_B = 0.23 — Q^2 = 5.9 GeV^2, x_B = 0.35

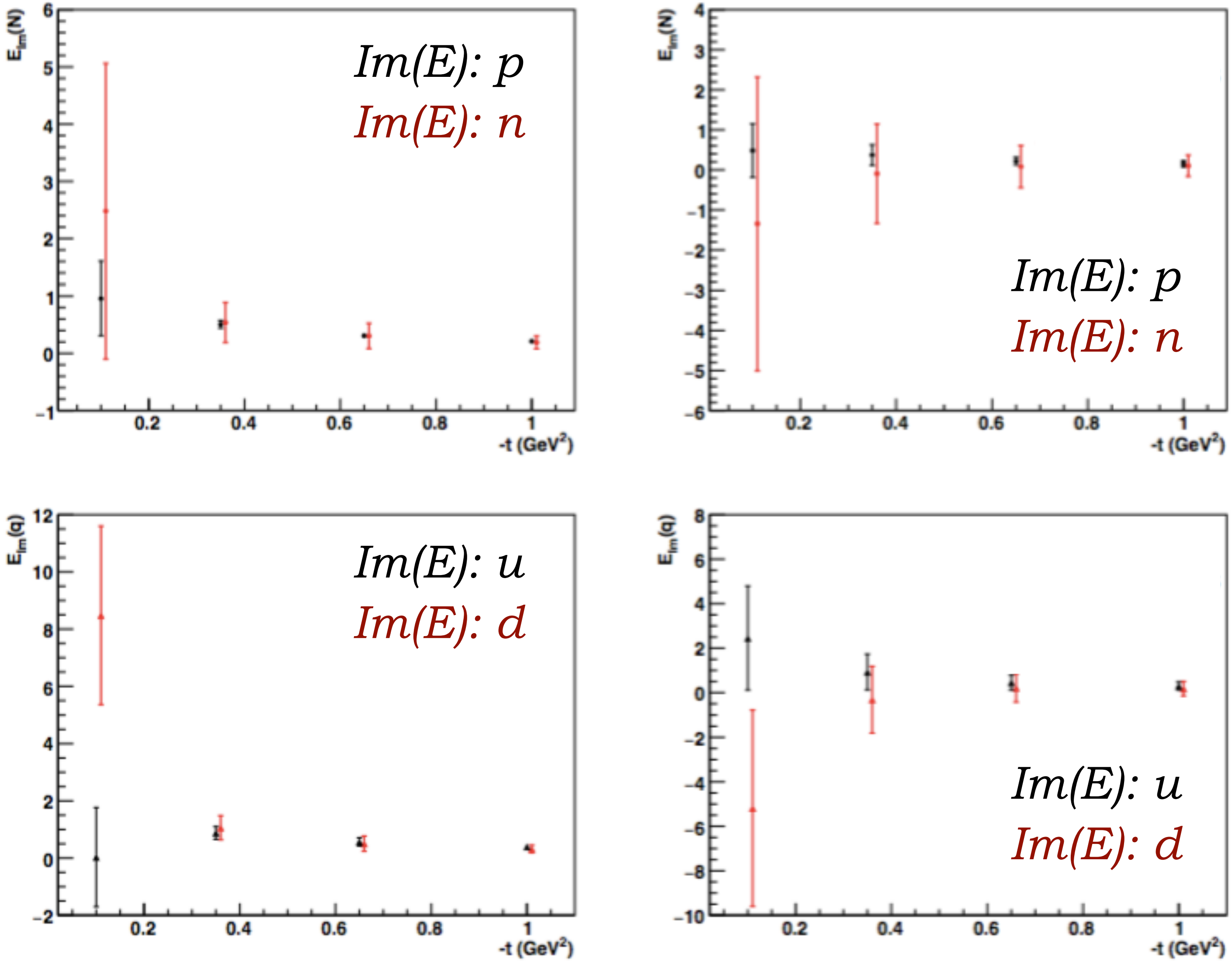

Projections for *Im(E)* neutron and proton and up and down CFFs extracted from approved and conditionally-approved CLAS12 experiments.

VGG fit (M. Guidal)

Luca Colaneri, Nabil Chouika (PARTONS)

DVCS beam-spin asymmetries at EIC

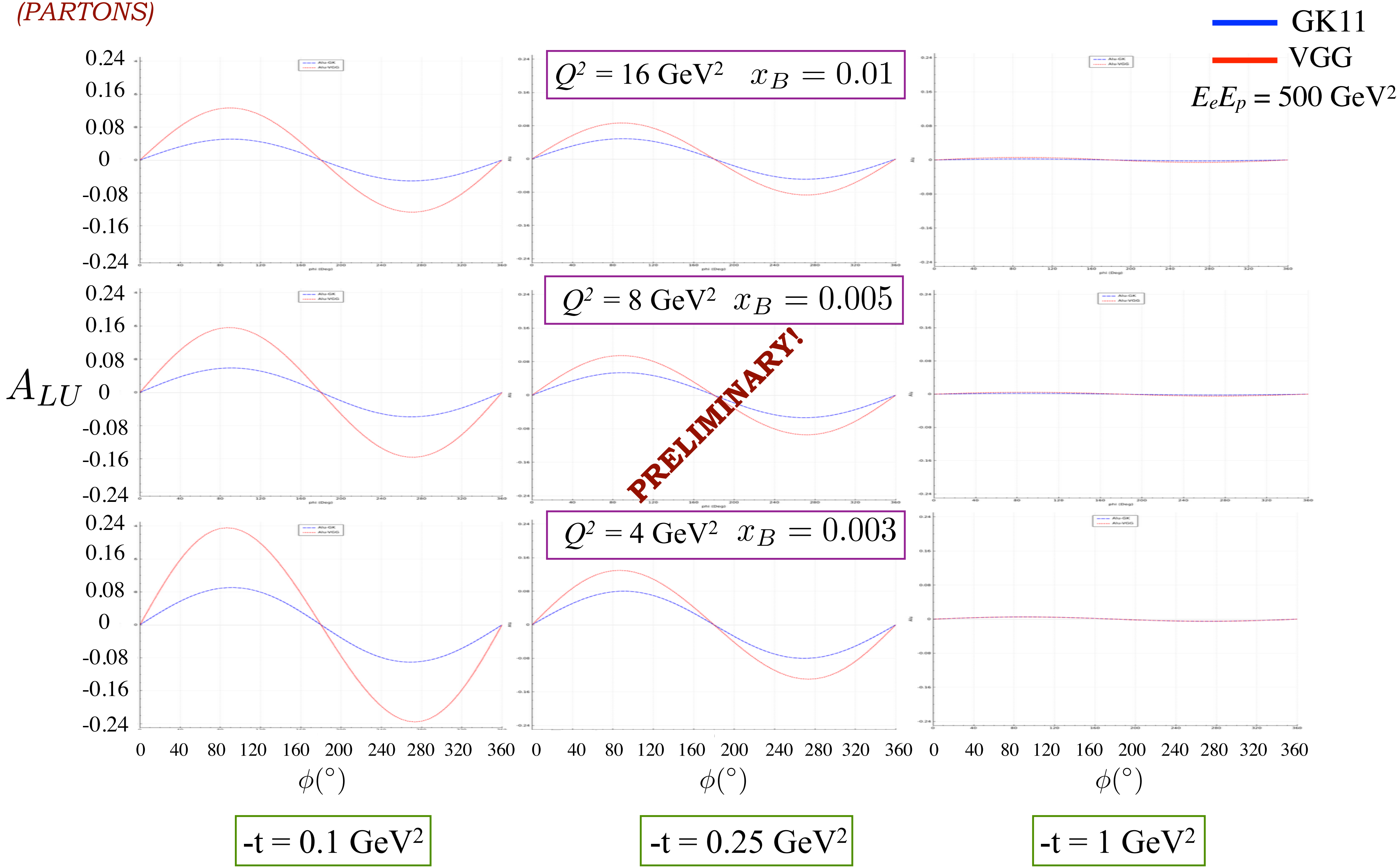

Summary

- **JLab at 6 GeV**: cross-section, single- and double-spin asymmetries in proton DVCS and a first measurement on neutron DVCS

  - Indications that factorisation holds at the low Q^2 kinematics of JLab,
  - constraints on a number of CFFs,

  → At LO-LT, tomographic picture of the nucleon in the valence region begins to emerge

  - importance of higher order / higher twist becomes evident in high-precision measurements.

- **JLab at 12 GeV** (11 GeV too halls A, B and C): new region of phase space at wider kinematics in the valence region. High luminosity, high precision.

- **DVCS measurements** are a flagship part of the experimental programme:first experiments in Hall A and with CLAS12.

- Approved experiments aimed at greatly **constraining CFF fits** in global analyses of DVCS on the proton, neutron and nuclear targets.

- Tomography of the quark-gluon sea will await a **high-luminosity EIC**.

Thank you

Jefferson Lab: 6 GeV era

CEBAF: Continuous Electron Beam Accelerator Facility.

- Energy up to ~6 GeV
- Energy resolution $\delta E/E_e \sim 10^{-5}$
- Longitudinal electron polarisation up to ~85%

Hall A:

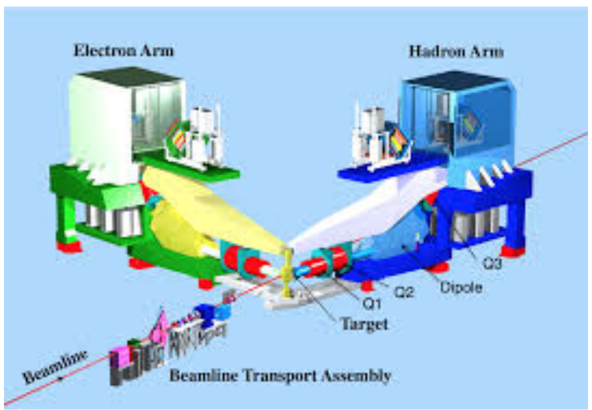

- High resolution($\delta p/p = 10^{-4}$) spectrometers, very high luminosity.

Hall B: CLAS

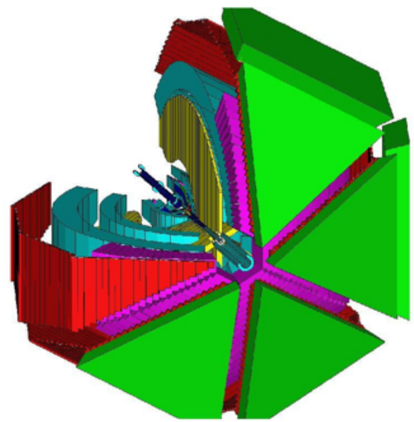

- Very large acceptance, detector array for multi-particle final states.

Hall C:

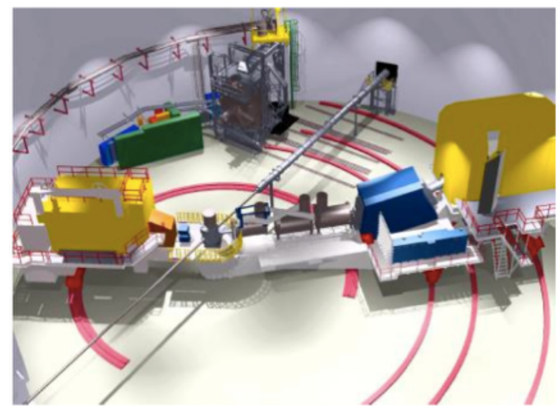

- Two movable spectrometer arms, well-defined acceptance, high luminosity

Jefferson Lab: 12 GeV era

- Maximum electron energy: 12 GeV to new Hall D
- 11 GeV deliverable to Halls A, B and C

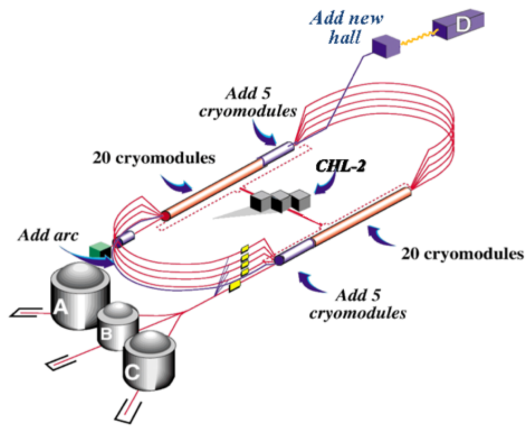

Hall A: High resolution spectrometers, large installation experiments

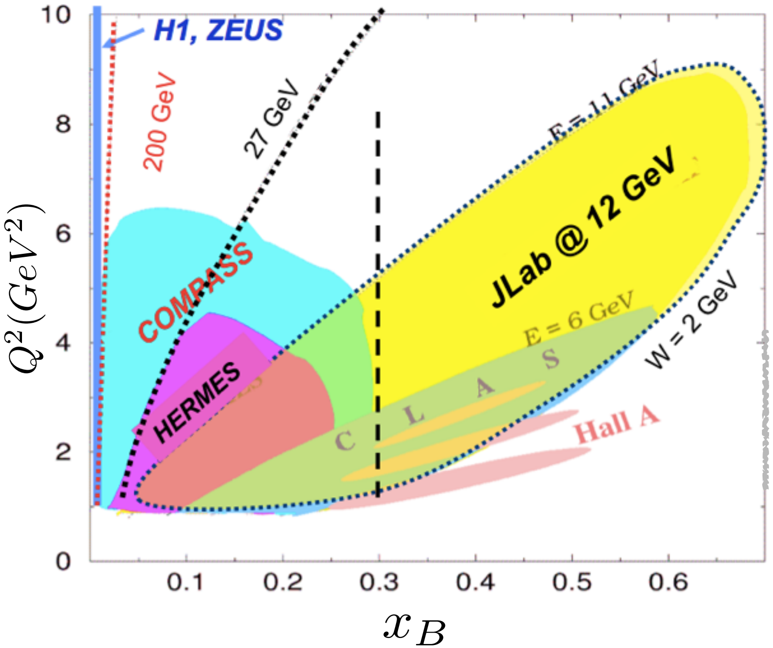

Hall B: CLAS12

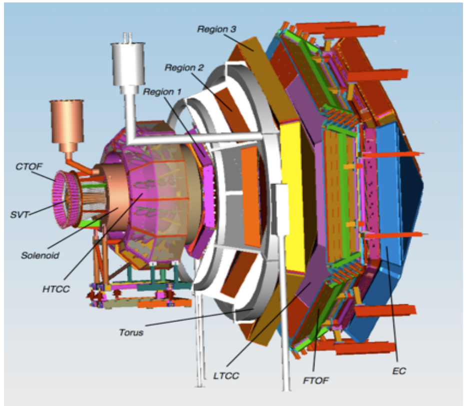

Very large acceptance, high luminosity

Hall D: 9 GeV tagged polarised photons, full acceptance detector

Hall C:

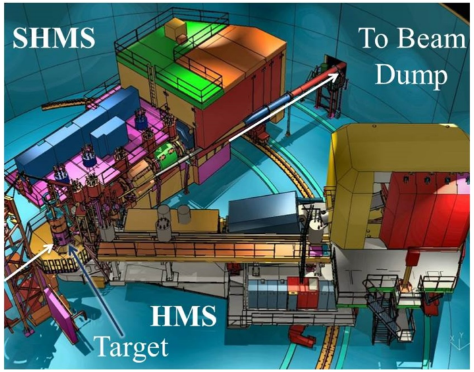

Super-high Momentum Spectrometer added, very high luminosity

Hall A

Rosenbluth separation of $DVCS^2$ and BH-DVCS terms

- Rosenbluth separation of the $DVCS^2$ and the BH-DVCS interference terms in the cross-section is possible, NLO and higher-twist required.

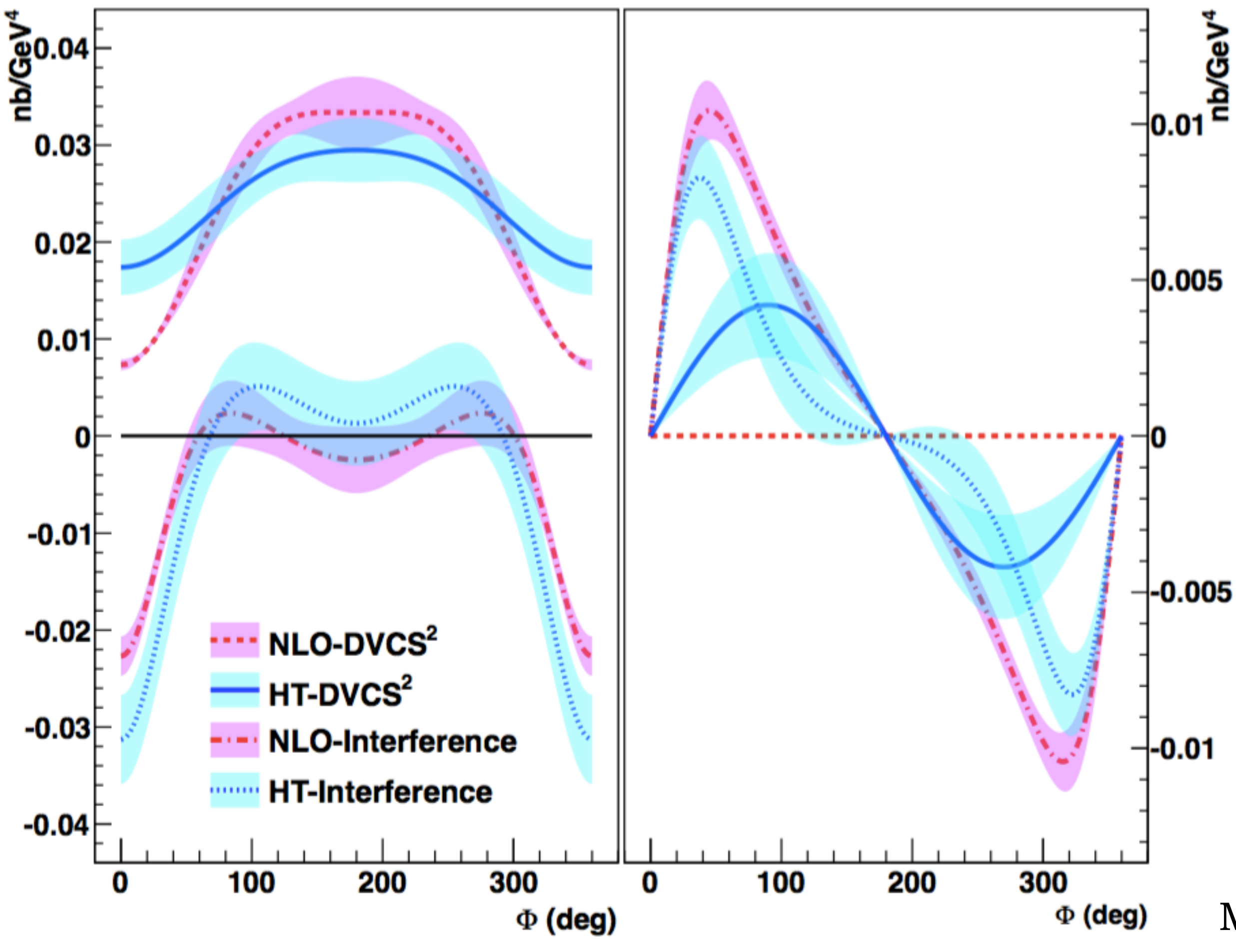

- Significant differences between pure DVCS and interference contributions.
- Helicity-dependent cross-section has a sizeable $DVCS^2$ contribution in the higher-twist scenario.
- Separation of HT and NLO effects requires scans across wider ranges of Q^2 and beam energy: JLab12!

M. Defurne *et al*, arXiv:c